Global and Planetary Change 170 (2018) 146–162

Contents lists available at ScienceDirect

Global and Planetary Change

journal homepage: www.elsevier.com/locate/gloplacha

Research article

Annual cycle of temperature trends in Europe, 1961–2000

Lucie Pokorná[a,b,*], Monika Kučerová[b], Radan Huth[a,b,c]

[a] Department of Physical Geography and Geoecology, Faculty of Science, Charles University, Prague, Czechia
[b] Czech Academy of Sciences, Institute of Atmospheric Physics, Prague, Czechia
[c] Czech Academy of Sciences, Global Change Research Institute, Brno, Czechia

ARTICLE INFO

Keywords:
Climate change
Maximum temperature
Minimum temperature
Temperature trend
Annual cycle
Europe

ABSTRACT

Recent global warming has not been ubiquitous: there are seasons, regions, and time periods with negligible or even negative air temperature trends (frequently referred to as warming holes). This paper presents a novel method enabling a proper localization of specific trend events, such as periods of warming holes, of a particularly strong warming, and of rapid transitions of trend amplitudes during the calendar year. The method consists in analyzing trends for periods of a given length (10 to 90 days) that are sliding over the year with a one day step. This allows a detailed description of the annual cycle of trends. The analysis is conducted for daily maximum and minimum temperature at 135 stations in Europe in 1961–2000. Despite an overall warming in Europe, several warming holes are uncovered during various parts of the year, not only in autumn when a warming hole has already been reported. The autumn warming hole concentrates in Eastern Europe, but it changes its strength and spatial extent: it spreads into Western Europe in September and retreats to Eastern Europe in November when it intensifies especially north of the Black Sea. Three shorter warming holes are detected: In February and March, cooling occurs in the Eastern Mediterranean and Iceland, while in early April, cooling is detected over Central, Southern, and Southeastern Europe. Another large-scale cooling occurs in Central, Northern, and Northwestern Europe in mid-June. The periods of strongest warming occur around the middle of January in Eastern Europe, in early March over almost entire Europe, and in mid-May and early August mainly over Central and Western Europe. Cluster analysis of stations with respect to the annual cycles of trends demonstrates a spatial coherence of the trends; the lack of spatial coherence points to local peculiarities or data problems of individual stations. The method of sliding seasons proves to be much more effective in the identification and localization of notable trend events than the ordinary approach of trend detection for fixed calendar seasons and/or months.

1. Introduction

The notable change of global mean temperature since the beginning of the industrial era is well known and widely documented, and so is the temperature change in both hemispheres and on the continental scale (e.g. Karl, 1993; Jones and Moberg, 2003; Hartmann, 2013.

The regional manifestation of global climate change does not often follow the behavior of global mean temperature; trends in surface temperature are uniform neither geographically nor during the year. No temperature change or even cooling occurred in some regions in various parts of year during the second half of the 20th century (Easterling, 1997; Jones and Moberg, 2003). For the periods and areas of non-warming and cooling, the term 'warming holes' was coined by Pan et al. (2004). The first warming hole explicitly described and discussed was the summer and autumn cooling over central and southeastern United States (Cavanaugh and Shen, 2014; Drijfhout et al., 2012; Rogers, 2013; Wang et al., 2009). Signatures of other warming holes that occurred in various seasons were uncovered in Canada (Zhang et al., 2000), Mexico (Cavanaugh and Shen, 2014), China (Hu et al., 2003), Southeast Asia (Jones, 1995), South Africa (Kruger and Shongwe, 2004), and Chile (Falvey and Garreaud, 2009), as well as in Europe (for relevant references, see the next paragraph). Unlike the U.S. warming hole, most of the other warming holes were not analyzed and discussed in any more detail, and were even only displayed without being explicitly mentioned in many studies.

In Europe as a whole, the warming since the 1950s was faster in comparison with the global temperature in all seasons (van Oldenborgh et al., 2009). The largest increase in European mean temperature was detected in winter and spring, amounting to 0.5 to 1.0 °C per decade during 1977–2001 (Jones and Moberg, 2003). Nevertheless, the

* Corresponding author at: Department of Physical Geography and Geoecology, Faculty of Science, Charles University, Prague, Czechia.
E-mail address: pokorna@ufa.cas.cz (L. Pokorná).

https://doi.org/10.1016/j.gloplacha.2018.08.015
Received 28 December 2017; Received in revised form 15 August 2018; Accepted 21 August 2018
Available online 24 August 2018
0921-8181/

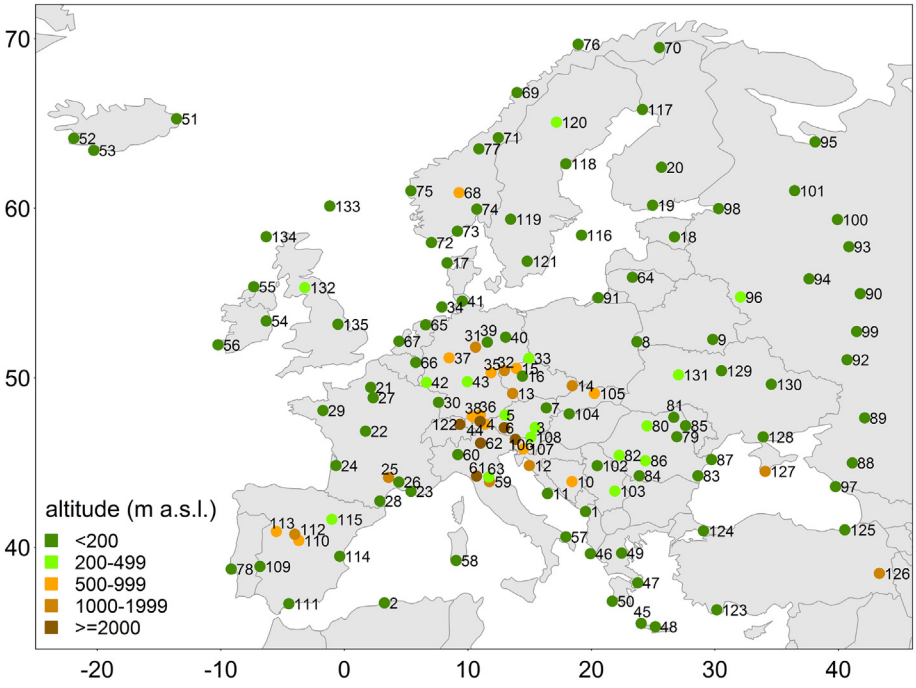

Albania
1. SHKODRA
Algeria
2. ALGER
Austria
3. GRAZ
4. INNSBRUCK
5. SALZBURG
6. SONNBLICK
7. WIEN
Belarus
8. BREST
9. VASILEVICI
Bosnia and Herzegovina
10. SARAJEVO
Croatia
11. HVAR
12. ZAVIZAN
Czechia
13. CHURANOV
14. LYSA HORA
15. MILESOVKA
16. PRAHA
Denmark
17. VESTERVIG
Estonia
18. TARTU
Finland
19. HELSINKI
20. JYVASKYLA
France
21. BEAUVAIS-TILLE
22. DEOLS
23. MARSEILLE
24. MERIGNAC
25. MONT-AIGOUAL
26. NIMES
27. PARIS
28. PERPIGNAN
29. RENNES
30. STRASBOURG
Germany
31. BROCKEN
32. FICHTELBERG
33. GORLITZ
34. HELGOLAND
35. HOF
36. HOHENPEISSENBERG
37. KAHLER ASTEN
38. KEMPTEN
39. MAGDEBURG
40. POTSDAM
41. SCHLESWIG
42. TRIER
43. WURZBURG
44. ZUGSPITZE
Greece
45. CHANIA
46. CORFU
47. HELLINIKON
48. HERAKLION
49. LARISSA
50. METHONI
Iceland
51. DALATANGI
52. REYKJAVIK
53. VESTMANNAEYJAR
Ireland
54. DUBLIN
55. MALIN HEAD
56. VALENTIA
Italy
57. BRINDISI
58. CAGLIARI
59. CAMPIGNA
60. MILAN
61. MONTE CIMONE
62. PAGANELLA
63. SAN CASSIANO
Lithuania
64. SIAULIAI
Netherlands
65. EELDE
66. MAASTRICHT
67. VALKENBURG
Norway
68. ABJORSBRATEN
69. GLOMFJORD
70. KARASJOK
71. KJOBLI I SNAASA
72. LINDESNES FYR
73. LYNGOR FYR
74. OSLO BLINDERN
75. TAKLE
76. TROMSO
77. VAERNES
Portugal
78. LISBOA
Romania
79. BACAU
80. BISTRITA
81. BOTOSANI
82. CARANSEBES
83. CONSTANTA
84. CRAIOVA
85. IASI
86. RAMNICU VALCEA
87. SULINA
Russia
88. ARMAVIR
89. CIMLJANSK
90. ELATMA
91. KALININGRAD
92. KAMENNAJA-STEP
93. KOSTROMA
94. MOSCOW
95. ONEGA
96. SMOLENSK
97. SOTCHI
98. ST. PETERSBURG
99. TAMBOV
100. VOLOGDA
101. VYTEGRA
Serbia
102. BELGRADE
103. NIS
Slovakia
104. HURBANOVO
105. POPRAD
Slovenia
106. KREDARICA
107. NOVA VAS
108. SMARTNO
Spain
109. BADAJOZ
110. MADRID
111. MALAGA
112. NAVACERRADA
113. SALAMANCA
114. VALENCIA
115. ZARAGOZA
Sweden
116. GOTSKA SANDON
117. HAPARANDA
118. HARNOSAND
119. KARLSTAD
120. STENSELE
121. VAEXJOE
Switzerland
122. SAENTIS
Turkey
123. FINIKE
124. ISTANBUL
125. RIZE
126. VAN
Ukraine
127. AI-PETRI
128. ASKANIIA NOVA
129. KIEV
130. POLTAVA
131. SHEPETIVKA
United Kingdom
132. ESKDALEMUIR
133. LERWICK
134. STORNOWAY
135. WADDINGTON

Fig. 1. Map and list of stations with their altitude (in colour).

seasonality of long-term temperature changes varies regionally: (i) warming since the 1960s was faster in spring than in winter over considerable parts of Central, Southeastern and Southwestern Europe (de Luis et al., 2014; Dumitrescu et al., 2015; El Kenawy et al., 2012; Serquet et al., 2011); (ii) summer warming dominated in Southeastern Europe, while near zero or slightly decreasing trends were detected there in winter and autumn (Brázdil, 1996; Feidas et al., 2004; Klein Tank et al., 2005; Mamara et al., 2016); and (iii) the absence of warming was observed in many regions in summer and autumn (Bajat et al., 2016; Brázdil et al., 2009; de Luis et al., 2014; del Río et al., 2007; Domonkos and Tar, 2003; El Kenawy et al., 2012; Franke et al., 2004; Huth and Pokorná, 2005; Jones and Moberg, 2003; Klein Tank et al., 2005; Moliba et al., 2006; Scherrer et al., 2012; van Oldenborgh et al., 2009; Wibig and Glowicki, 2002; Xoplaki et al., 2005). Studies on temperature trends in Europe typically focus on individual countries or small regions, use different methodologies, and analyze periods of different lengths. Despite a large number of individual studies it is, therefore, hardly possible to create a coherent overview on the spatial distribution of temperature trends over the whole of Europe.

Most studies analyze seasonal trends, while only a few trend studies have been conducted in a monthly resolution (Brázdil et al., 2009; del Río et al., 2007; Domonkos and Tar, 2003; Keevallik and Russak, 2001; Mamara et al., 2016; Serra et al., 2001; Scherrer et al., 2006; Weber et al., 1994). One of the reasons for using fixed seasons and/or months is a simplicity of such detection studies. The analyses of trends document strong variations of trend magnitudes, and even changes in the sign of trends, from one season to another. Strong contrasts between trends in adjacent months are a typical feature rather than an exception; they indicate that seasonal and even monthly trends are not sufficient for uncovering and fully describing the behavior of trends throughout year. Thus the need for a comprehensive and more precise study of trends, allowing for their better localization during the

calendar year as well as in space, is obvious.

In this paper we present a completely new approach to a full description of temperature trends on a subseasonal scale during the calendar year and apply it to daily maximum and minimum temperatures in Europe. The essence of our approach is that trends are calculated for sliding seasons of different lengths. This allows a detailed annual cycle of trends to be described and notable manifestations of trends, such as fast warmings and warming holes, to be temporally localized within the year with the accuracy of one day. Our choice of the lengths of subseasons, 10 to 90 days, reflects findings by Serra et al. (2001), Wibig and Glowicki (2002), and Moliba et al. (2006) that trends computed from only one calendar day in each year exhibit a very high day-to-day variability and are mostly statistically insignificant, whereas trends of 10-day periods undergo considerably lower day-to-day variability and attain statistical significance, while still capturing sudden changes of a trend magnitude. Longer (30- and 90-day) sliding seasons enable a direct comparison with other studies, which are almost exclusively available for calendar months and climatological 3-month seasons.

The objectives of the study can thus be summarized as follows: (i) to present and apply the new method for detection of the annual cycle of trends, consisting in separate trend analyses in overlapping sliding periods, and demonstrate its utility and benefits, and (ii) to provide a coherent description of the spatial and temporal distribution of temperature trends over the whole of Europe. Such a descriptive analysis is necessary prior to any subsequent research into causes of various trend features and patterns that we detect; such research, however, goes beyond the scope of the present paper.

2. Data and methods

2.1. Climatic data

The study is conducted for daily maximum (TX) and minimum (TN) air temperature at 2 m (in °C) at 135 stations in Europe and its close proximity (Fig. 1) in period 1961–2000. Data for 133 stations are retrieved from the European Climate Assessment & Dataset (ECA&D, Klein Tank, 2002; Klok and Klein Tank, 2009). This dataset is complemented with two mountain stations in Czechia (Churáňov and Lysá hora), which were obtained from the Czech Hydrometeorological Institute. The stations were selected to be approximately evenly distributed over the research area. We performed basic quality control of the daily data; suspect values were discarded or, in rare cases, corrected (e.g. missing decimal point). Homogeneity tests were not applied. Only stations with < 2.5% of missing daily data are considered; we did not attempt to fill in gaps. The density of stations is kept higher in Central Europe and around the Alps because of complex orography there; on the other hand, no data are available from Poland, Hungary, and Bulgaria.

2.2. Methods

All the analyses are conducted for mean values of sliding seasons. The sliding seasons of the lengths of 10, 20, 30, 60, and 90 days are formed by moving the time window by a one-day step. 365 sliding seasons are thus formed for each climatic variable and each sliding season length in every year. 29th February is excluded from calculations for simplicity. The mean of a particular sliding season is computed only if > 80% of daily values are available for that season; otherwise, the mean value is considered missing.

As all sliding seasons contain an even number of days, they have no middle day; we label them in graphs by the day that precedes their middle day. For example, the 10-day sliding season from January 11 to 20 is labeled as January 15. To keep the length of the series the same (40 years) for each sliding season regardless of their position in year, and to make use of all data (that is, not to lose the data from the beginning of the first year and the end of the last year), the mean values for sliding seasons straddling the end of year are calculated from days from the same year. For example, the mean of the 90-day sliding season from November 30 to February 27 is calculated as a mean from January 1 to February 27 and from November 30 to December 31 of the same year.

In the next step, trends of TX and TN for sliding seasons are assessed by linear least-squares regression. The magnitudes of trends determined by the non-parametric method of the median of pairwise slopes (Lanzante, 1996) differ from them only marginally, which is in accord with Huth and Pokorná (2004), and are not shown here for the sake of brevity. The statistical significance of trends at the 5% level is determined by Mann-Kendall test (Sneyers, 1990); *t*-test gives very similar results and is not reported here either. The use of Mann-Kendall trend test is justified by the fact that the number of time series with significant positive autocorrelation is well below the 5% level of global significance. Values of lag-1 autocorrelation of detrended time series of TX and TN averaged over sliding seasons are provided in supplementary material, Fig. S1. Trends are calculated for all the 365 sliding seasons of each length; the annual cycle of trend magnitudes with a daily step is thus obtained. Note that one would obtain four values of trend only if common climatological 3-month seasons were analyzed instead of sliding seasons, which would not allow the annual cycle of trends to be assessed.

We present and discuss both significant and insignificant trends to get a complete picture of the distribution of trends during the year. As discussed by Nicholls (2001) and Moberg and Jones (2005), the neglect of insignificant trends may lead to the loss of a substantial amount of valuable information. We must, however, be aware that more noise is present in smaller temporal (short sliding seasons) and spatial (individual stations) scales, which limits their interpretation. Therefore, we focus on the interpretation of trends over objectively defined regions.

A comprehensive overview of the behavior of trends over the whole of Europe is provided by clustering stations according to the annual cycle of temperature trends. Raw (non-standardized) values of trends of TX and TN for 365 sliding seasons enter cluster analysis. We use the "Partition over Medoids" clustering algorithm (Kaufman and Rousseeuw, 1990); this is a non-hierarchical method, which is in fact a robust version of k-means clustering. We find it to be superior to hierarchical methods since the latter tend to separate stations with higher trend amplitudes regardless of the overall similarity of the annual cycles of trends. This results in a typical snowballing effect, reported in various clustering studies: several small clusters containing one or two stations are formed together with one very big cluster (e.g., Huth et al., 1993); we deem such a behavior is undesirable in this analysis, too. The cluster analysis is performed using the "cluster" package within the "R" environment (The R Project for Statistical Computing, http://www.r-project.org/). Results of cluster analysis are only displayed for 30-day sliding seasons for the sake of brevity.

The number of clusters is determined subjectively, the geographical coherence of clusters and the between-cluster diversity together with the within-cluster similarity of annual cycles of trends being the most relevant criteria. Fig. 2 illustrates the selection of the number of clusters for TX: Five clusters represent a fairly suitable distribution of stations. For six clusters, a new (purple) cluster forms another quite coherent region comprehending stations from the green, red, and blue clusters of the five-cluster solution, which are located in Romania, other parts of the Balkan Peninsula, and the northern Black Sea coast. The annual cycle of trends in the purple cluster is distinct from the red cluster thanks to a smaller warming in winter and near-zero trends in April and June. The annual cycles of trends in the turquoise cluster, which is geographically incoherent, containing stations in Iceland and southeastern Europe, are similar in its both distant parts (see Section 3.3 for more details), which justifies their assignment to a common cluster. The formation of the seventh (pink) cluster does not bring new information: The pink cluster is geographically incoherent, containing several

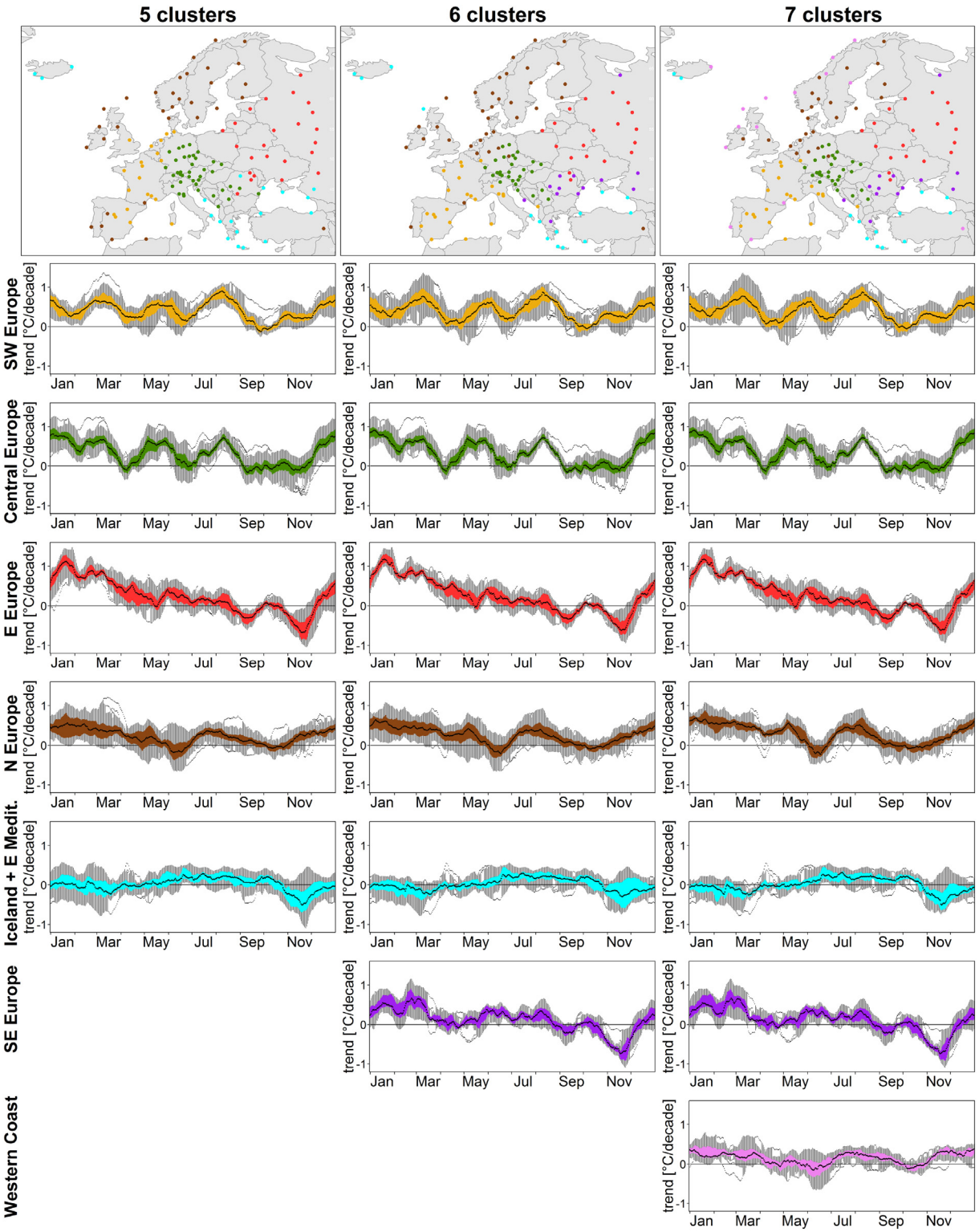

Fig. 2. Division of Europe into 5, 6, and 7 clusters for TX trends and 30-day sliding seasons. Maps show the assignment of stations to clusters. The graphs of annual cycles of trends for individual clusters (shown in the same colour as on the maps) are composed of boxplots for individual days summarizing the stations within the clusters: the thick black line is the median, the colored strip (boxes) represents central 50% of stations (lower to upper quartile), whiskers (forming grey areas around the colored strips) indicate trends within 1.5 times interquartile range from the upper and lower quartile, and dots indicate outliers.

coastal stations from different parts of Europe, and its annual cycle of trends is half way between the blue and brown clusters. So the optimal number of clusters is set to 6 for TX. An analogous procedure (not shown) leads to 5 clusters for TN. We applied the clustering procedure also to trends normalized by the interannual standard deviation (not shown); resulting clusters are very similar to those presented here, which gives confidence to the robustness of clusters.

Although we concentrate on absolute trends, trends normalized by the interannual standard deviation are briefly discussed in Section 3.6.

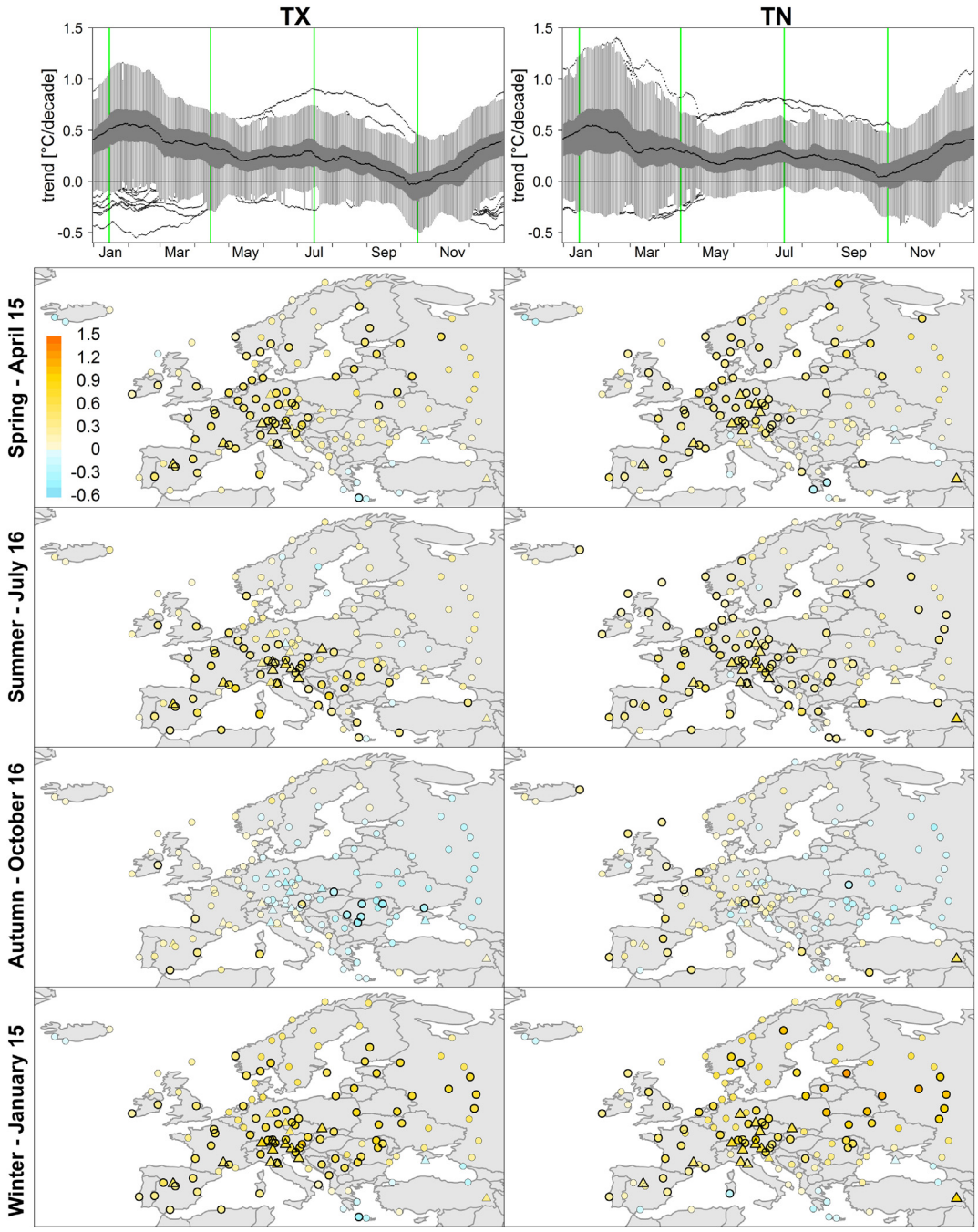

Fig. 3. Maps: Trends of TX and TN for 90-day sliding seasons corresponding to standard climatological seasons. The magnitude of trends (in °C per decade) is indicated by colour; stations with trends significant at the 5% level are highlighted by black rims. Stations below/above 1000 m a.s.l. are marked with circles/triangles. Boxplots at the top summarize trends at all stations for 90-day sliding seasons analogously to Fig. 2. Green vertical lines show the position of the central days of climatological seasons, for which the maps are shown.

3. Results

3.1. Trends for climatological seasons

Temperature trends are first displayed for 90-day sliding seasons that correspond to ordinary climatological seasons: 15 January for winter, 15 April for spring, 16 July for summer, and 16 October for autumn (Fig. 3). One can clearly see a warming at the majority of stations in winter, spring, and summer, which is strongest in Eastern Europe and the Alps in winter, and a cooling in autumn occurring in most of Europe except its western and northwestern part. This picture of seasonal trends agrees with what many studies on temperature trends in Europe, referenced in Sec. 1, report with varying geographical coverage and time period. Comparing with the U.S. autumn warming hole documented in the period 1950–2000 (Wang et al., 2009), the magnitude of negative trends at stations in Central and Eastern Europe is similar: typically from −0.2 to −0.8 °C in case of TN and from −0.2 to −1.2 °C for TX during four decades 1961–2000, while in the U.S. between −0.3 to −0.9 °C over most areas. Greatest temperature change per 40 years of below −1.0 °C for TN and − 1.5 °C for TX was detected at individual stations in Romania, Ukraine, Belarus, and Russia, which corresponds to the magnitude of cooling in southeastern Nevada and southwestern South Dakota (below −1.5 °C per 50 years). Trends for 30-day sliding seasons, corresponding to calendar months, can be found

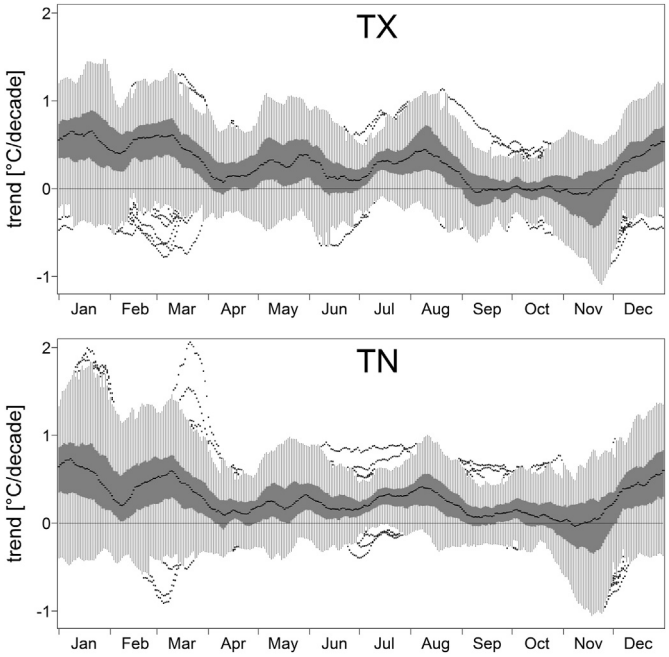

Fig. 4. Boxplots summarizing trends of TX and TN for 30-day sliding seasons at all 135 stations: median (black line), upper and lower quartile (boxes, dark grey), range of trends within 1.5 times interquartile range from the upper and lower quartile (whiskers, light grey), outliers (dots).

in supplementary material, Figs. S2 and S3.

3.2. Overview of sliding trends

The magnitude of trends for 30-day sliding seasons at all stations is summarized in box-and-whisker plots in Fig. 4 (analogous graphs for other lengths of sliding seasons are included in the supplementary material, Fig. S4). Europe as a whole generally warms during almost the whole year; however, for any 30-day period, there are stations where a cooling occurs. The same holds for any length of sliding seasons from 10 to 90 days. The negative trends in both TX and TN are least numerous (that is, the warming is most widespread) in July and August. The cooling is most extensive in autumn, in November in particular, appearing at more than half of the stations for sliding seasons of up to 60 days long. The spread of trends across Europe (the difference between the highest and lowest trend displayed as the length of whiskers) oscillates around 2 °C per decade throughout the year for 30-day seasons; it is largest for TN in winter and lowest for both TX and TN in July, September, and October.

Another look at the overall behavior of temperature trends in Europe is provided in Fig. 5, which shows the percentage of stations with significant and insignificant positive and negative trends for sliding seasons of different lengths. We can clearly see that both TX and TN decrease somewhere in Europe at any time during the year on all time scales from submonthly (10 days) to seasonal. The changes in the number of stations with cooling/warming are very fast, especially in the beginning of April, around the end of August, and near the end of November. For example, while daytime cooling (decrease in TX) for 10- and 20-day sliding seasons is present at slightly over 10% of stations still around 25 August, this number jumps up in the following couple of days, reaching about 55% on 1 September. The majority of trends are not significantly different from zero; as mentioned in Section 2.2, we follow the arguments by Nicholls (2001) and Moberg and Jones (2005) that even insignificant trends may – and should – be interpreted.

Three periods of prevailing cooling are detected in TX for 10-day sliding seasons: cooling is observed at more stations than warming in April, June and in several parts of autumn. On the other hand, warming is most geographically extensive in January, early spring, and in the second half of summer, when the dominance of warming is more pronounced for TN.

The increase of the length of sliding seasons leads to short-term variations being smoothed out. Whereas the periods of prevalent cooling and strongly prevalent warming can be observed for sliding seasons of up to a 30-day length, for 90-day seasons the picture changes to a consistent warming of both TX and TN, which is observed at > 80% of stations during the whole year with the exception of autumn. By limiting the analysis to 90-day sliding seasons, one would obviously lose substantial information about short periods of cooling in April and June; the notable warming significant at about 50% of stations near the middle of August would not be uncovered either. One can also see that trends in standard climatological seasons (displayed as vertical lines in the bottom graphs of Fig. 5) are not able to capture the variability of trends throughout a year: For example, summer trends in TN (corresponding to the sliding season centered on 16 July) indicate an extensive summer warming with over 60% of stations experiencing significant positive trends. This prevalence of significant positive trends weakens considerably, however, when one moves the sliding season a few days forward or backward; obviously, what is presented as summer trends may not be representative for entire summer. A similar argument applies to a prevalent cooling in TX in autumn (corresponding to the sliding season centered on 16 October).

3.3. Cluster analysis of sliding trends

The simultaneous presence of positive and negative temperature trends at any time during a year raises the question of how the annual cycle of trends varies in space. This is analyzed and displayed for 30-day sliding seasons. Individual stations are grouped by cluster analysis according to their annual cycles of trends; six and five clusters were found to be optimum for TX and TN, respectively, as described in Section 2.

Fig. 6 presents the classification of stations and the annual cycle of temperature trends for individual clusters. The classifications for the two temperature variables bear a noticeable similarity: grouped together both for TX and TN are stations e.g. in Scandinavia and Finland (brown clusters in Fig. 6), in Eastern Europe (red clusters), in Central Europe (green), in Iceland and parts of the Central and Eastern Mediterranean (turquoise), and in southwestern Europe (yellow). On the other hand, there are some marked differences between the clustering for TX and TN, such as a separate cluster in Southeastern Europe for TX (purple), a different assignment of stations in the British Isles and on the North Sea coast, in western France, as well as in northern Italy.

More details are provided in Fig. 7, which displays annual cycles of trends in TX for all individual stations, grouped by their membership to clusters and, for larger clusters, also geographically. Analogous information on TN trends can be found in Fig. S5 of the supplementary material.

Perhaps the most geographically coherent is the green cluster, joining stations with a relatively large warming from December to August and a notable warming hole, extending over almost entire autumn (Fig. 6). The warming is interrupted by two short periods of a reduced warming or even cooling at the beginning of April and in late June and another period of reduced warming in early February. This cluster covers mainly Central Europe (Germany, Austria, Switzerland, Czechia, Slovakia, Hungary, Slovenia, Croatia) and extends farther west towards France for TN, while farther southeast up to Bosnia and Herzegovina and Serbia for TX. The warming holes in July and autumn are less pronounced and the warming in February is smaller for TN than for TX. The warming in TN in autumn prevails mainly at the lowland (up to 800 m a.s.l.) stations in the Alps (Fig. S6 in supplementary material). Worth noting is a specific behavior of Graz where trends in TX are strongest (most positive) of all stations classified with the green cluster during most of year. This feature is particularly striking around the turn

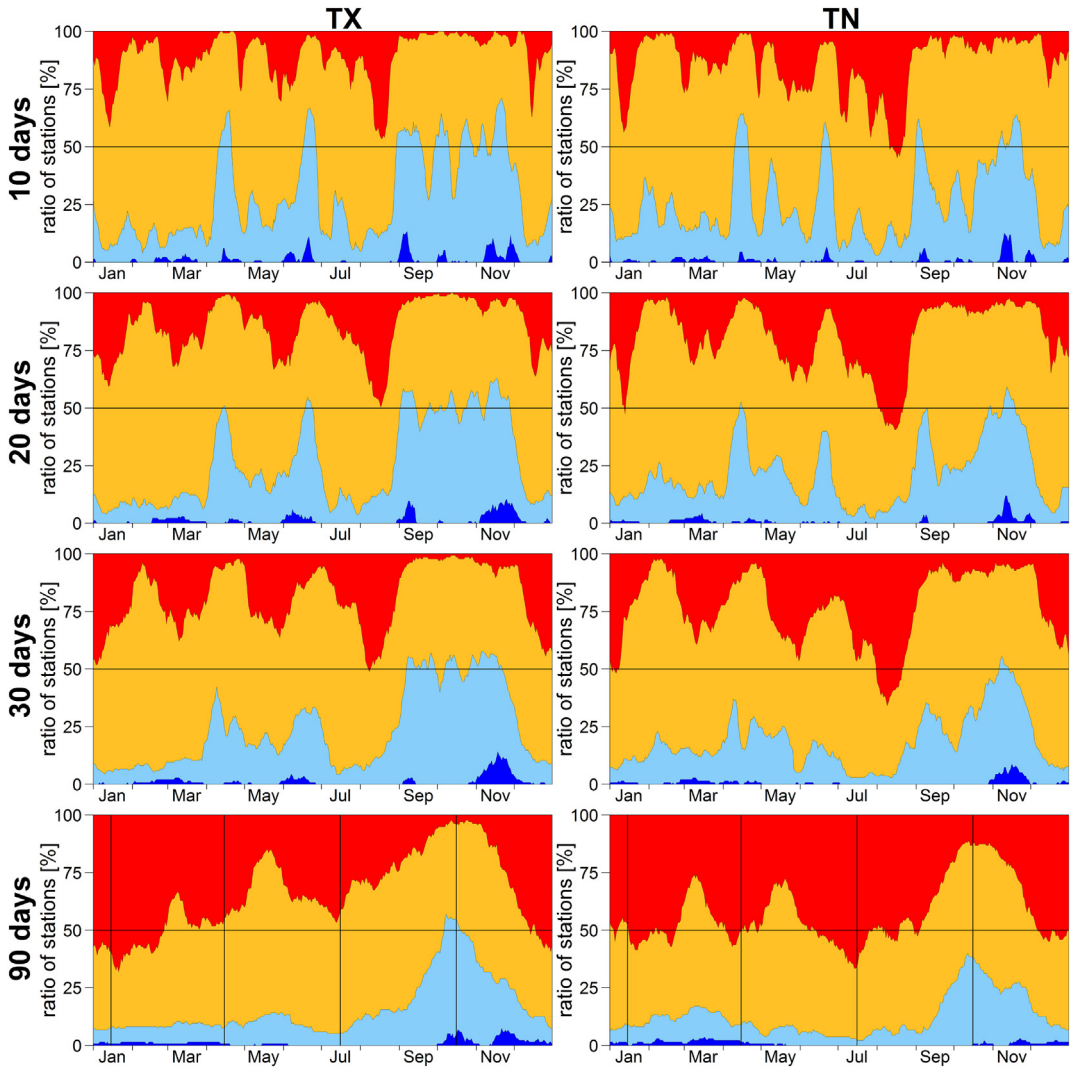

Fig. 5. Percentage of stations with significant positive (red), insignificant positive (yellow), insignificant negative (light blue), and significant negative (dark blue) trends in TX (left) and TN (right) for 10-, 20-, 30-, and 90-day sliding seasons (from top to bottom). Vertical lines in the bottom graphs indicate central days of standard climatological seasons.

of February and March and in September. It is not possible to judge from the data available whether these features are real manifestations of climate or result from a lack of representativeness of this station or its possible inhomogeneity. A behavior of temperature trends somewhat similar to the green cluster, but with less warming in winter and a considerably shorter autumn warming hole, which culminates in early October, is observed at the stations classified with the yellow cluster, covering Southwestern and Western Europe (France, Spain; see Fig. 6). Periods of strongest warming occur in early March, late May, and August, for the majority of stations. The periods of non-warming in April and June are less pronounced in comparison with Central Europe (green cluster). The variations of trend magnitudes during the year are stronger for TX than TN as a consequence of stations in the British Isles and the North Sea coast (Belgium, the Netherlands, Denmark, western coast of Norway) joining this cluster for TN, while stations farther eastwards in Central Mediterranean (Italy, Albania) joining it for TX. There is a noticeable heterogeneity within this cluster (Fig. 7): Stations in the interior of the Iberian Peninsula (Navacerrada, Badajoz, Madrid, Salamanca) differ from coastal stations in the Western Mediterranean (Valencia, Malaga, Alger) by a stronger warming in late February and March, as well as in early June and late July.

The brown cluster contains stations mainly from Northern Europe (Fig. 6); this cluster extends farther west (Norwegian coast, British Isles) for TX, for which also two sites in the Iberian Peninsula and one site in Turkey are attached, while it covers northern Russia and the Baltic states for TN. The cluster is characterized by a rather strong warming (stronger for TN) in the cold half-year (from November to mid-May) and also in high summer (July and August; stronger for TX). A notable cooling of TX at a majority of stations ($> 75\%$) occurs in June, and another non-warming period persists from September to October. The isolated stations (Perpignan, Lisbon, Van; Fig. 7) appear to be assigned to the brown cluster because of their large dissimilarity from other clusters rather than their close similarity to this cluster. A specific behavior of trends in TN occurs at stations in the Scandinavian interior and near the Gulf of Bothnia (Karasjok, Haparanda, Stensele, Jyväskylä; Fig. S5): a strong warming in late March, which exceeds TX trends at other Scandinavian stations by several tenths of °C per decade. This issue is discussed in more detail later in Sec. 3.5.

A pattern in temperature trends similar to the brown cluster can be found in Eastern Europe, represented by the red cluster, with the difference that the period of pronounced warming starts later (in December) and lasts until April (Fig. 6). This cluster extends farther northwestward for TX while farther southward for TN. The winter warming in this cluster is largest all across Europe, is stronger for TN, and is related to a very high interannual variability of temperature (for more details on the relation of the magnitude of trends to variability,

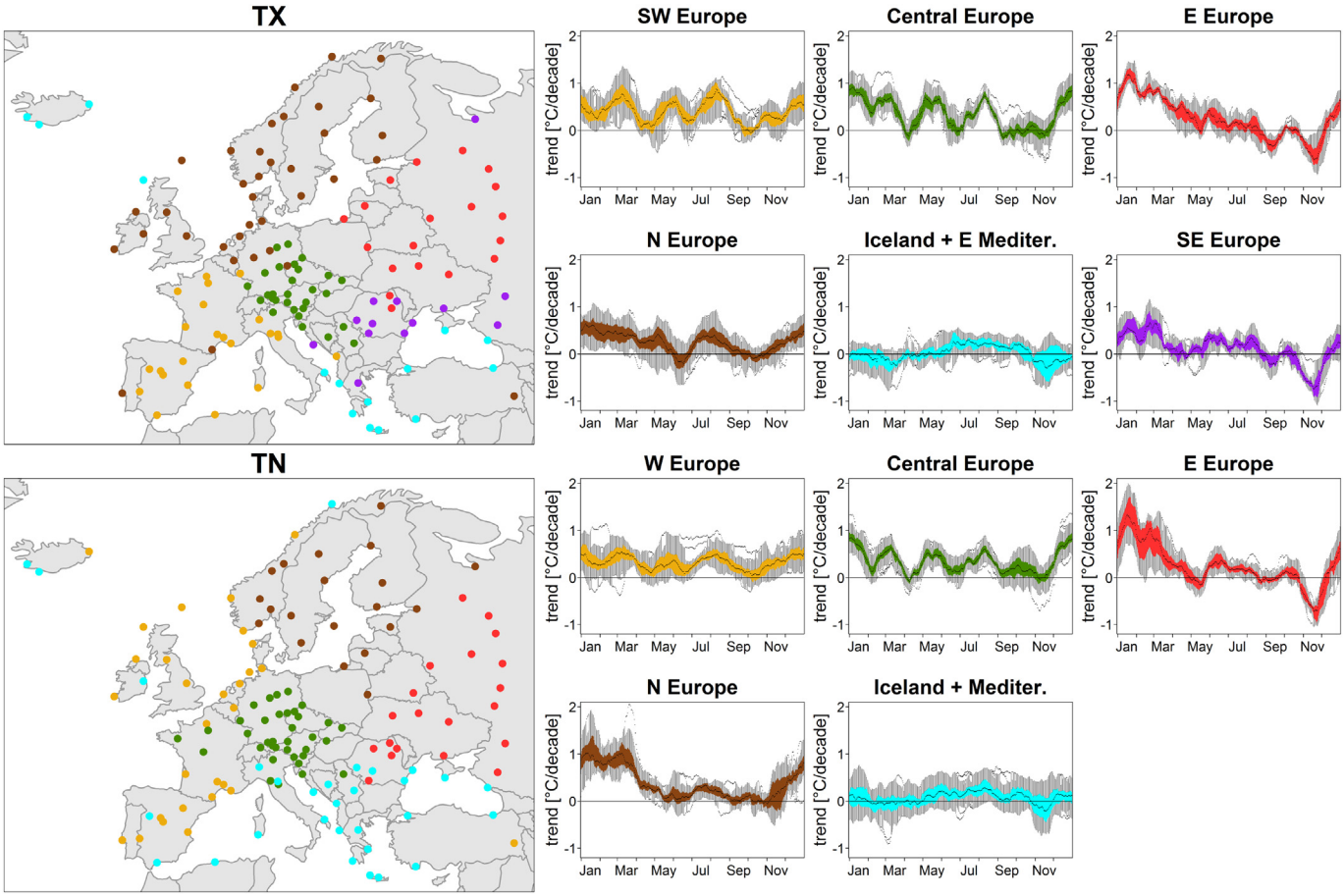

Fig. 6. Classification of stations for TX (top) and TN (bottom) and the annual cycle of trends in individual clusters (distinguished by colors), all for 30-day sliding seasons. The graphs are arranged in the same way as in Fig. 2.

see Sec. 3.6). Autumn is accompanied with cooling that appears at all stations in two waves; one in early September, which is barely noticeable in TN, and another, stronger, in November. The January warming is particularly strong for TN: it exceeds 1.5 °C per decade at several stations in Northeastern Europe and is by several tenths of °C per decade larger than the TX trends there (Figs. 7 and S5).

Stations from Southeastern Europe (mainly from Romania and the northern Black Sea coast) group together for TX only, forming the purple cluster (Fig. 6). This cluster represents a transition between Eastern Europe (red cluster) and the Eastern Mediterranean (turquoise cluster); most stations classified with the purple cluster for TX are assigned to the red or turquoise cluster for TN. Trends in this cluster are similar to the red cluster, however with lower magnitudes of trends in winter, with warming peaking in late February instead of January, and a longer period of reduced warming or non-warming that persists during almost entire spring. Note that although Onega (the northernmost Russian station) is assigned to the purple cluster, we display it in Fig. 7 together with the stations from the red cluster because of a geographical coherence.

The turquoise cluster combines stations from two regions distant from each other: The Central and Eastern Mediterranean and the Black Sea coast on one hand, and Iceland and one station in Scotland on the other (Fig. 6). For TN, this cluster extends into the western Mediterranean and contains one isolated station in northern Norway (Tromsø) in addition. This cluster differs from all the other clusters by a relatively low magnitude of trends. Warming concentrates in the warm half of year (May to September), while almost no warming is observed in the cold half-year; most Mediterranean stations in fact experience cooling from November to March (Fig. 7).

It is worth noting, particularly in the light of studies of the altitudinal dependence of temperature trends (Ceppi et al., 2012; Ohmura, 2012; Philipona, 2013; Rangwala and Miller, 2012), that there are no clear signatures that the annual cycles of trends might be influenced by the altitude or by surrounding terrain (plain, valley, mountain summit). The only notable exception is a significant autumn warming of TN at low-lying stations in the Alpine region (already mentioned above), which is not present at nearby mountain stations (Fig. S6). However, the station network analyzed here is not dense enough to demonstrate or dismiss the altitudinal dependence clearly. An analogous analysis focusing on denser station networks in mountainous regions is a planned extension of the current study.

3.4. Localization of warming holes

The following two subsections describe notable trend events, such as warming holes and periods of strong warming (peak warmings) and localize them within year. These events are characterized by maps of 30-day sliding trends for selected periods in Figs. 8 to 11. The full annual cycle of trends for 30-day sliding periods for both TX and TN can be enjoyed as an animation in supplementary material (Fig. S7).

Figs. 4 and 5 indicate that a relatively large proportion of stations undergo cooling in autumn, indicating a presence of a warming hole. Figs. 6 and 7 attribute the cooling mainly to the red and purple clusters, that is, to Eastern and Southeastern Europe, although a considerable number of stations in the green and turquoise clusters, that is, in Central Europe and the Eastern and Central Mediterranean, exhibit negative temperature trends in a part of autumn, too. This concurs with other studies on temperature trends in Europe, referred to in Section 1.

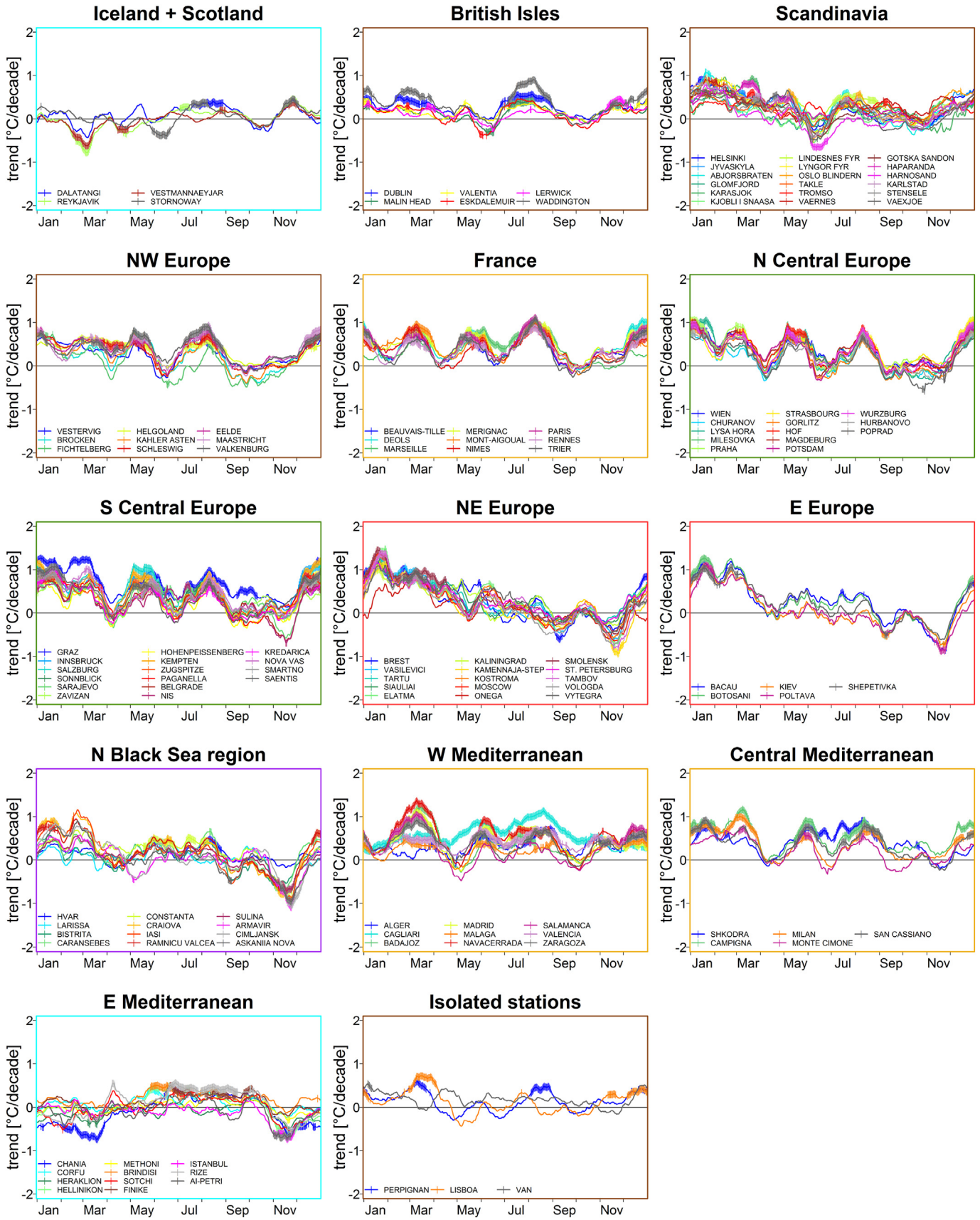

Fig. 7. Trends in TX for 30-day sliding seasons at individual stations (marked by different colors) arranged by their assignment to clusters (marked by colors of frames, which correspond to colors in Fig. 6). Large clusters are further divided geographically for the sake of clarity of display. Trends significant at the 5% level are highlighted by short vertical lines, which display as thick sections of curves.

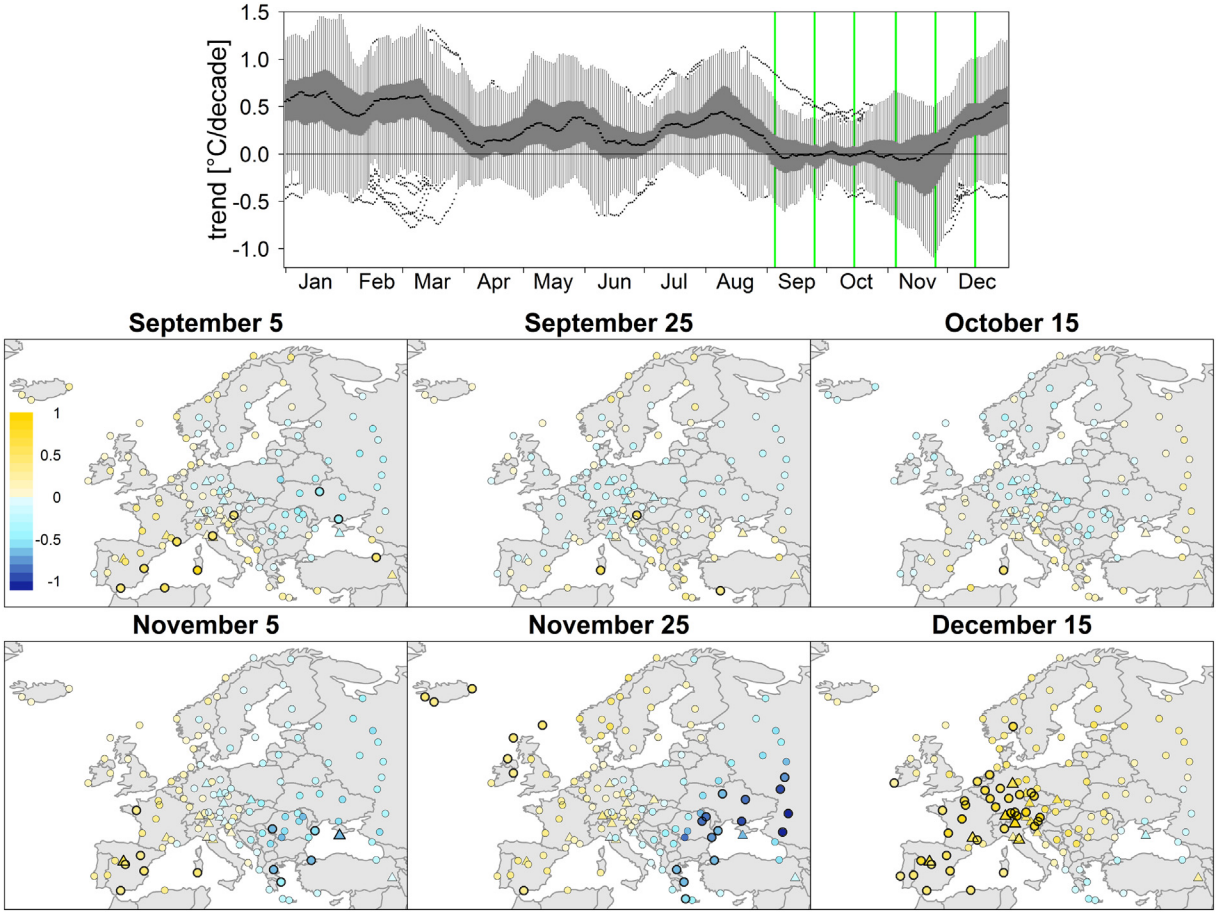

Fig. 8. Autumn warming hole. Boxplot as in Fig. 2. Green vertical lines show the position of the selected days. Maps as in Fig. 3 but for TX and for selected 30-day sliding seasons in autumn and early winter.

Here we attempt to localize the autumn European warming hole with a more precision both in space and within the annual cycle. Fig. 8 displays TX trends for 30-day sliding seasons in autumn and early winter separated by approximately 20 days, thus visualizing the temporal evolution of the spatial extent and position of the warming hole. The warming hole concentrates in Eastern Europe, but it changes its strength and spatial extent during its existence. In early autumn, it spreads into Western Europe, reaching its maximum extent in late September. It retreats to Eastern Europe in November when it intensifies especially north of the Black Sea. In December, the warming hole finally moves southeast and almost vanishes: the majority of Europe undergoes warming. The cooling in Eastern and Southeastern Europe comes in two waves: the weaker one in September and the stronger one, with more numerous negative trends and more frequent statistical significance, in November.

Sliding trends allow us to detect warming holes also in other seasons when the periods of non-warming are shorter. Figs. 6 and 7 suggest that warming holes, which are less spatially extensive than the autumn hole, occur in various parts of Europe. The spatial extent of such minor warming holes is documented in Fig. 9, displaying TX trends for 30-day sliding seasons, in which their spatial extent and/or magnitude attain maximum values. In mid-February, cooling occurs in the Eastern Mediterranean and Iceland; it lasts until early March when it culminates in Iceland. This cooling appears to be the major reason for these two distant regions being joined in one cluster. Another warming hole, with a large spatial extent, appears in early April over Central, Southern, and Southeastern Europe. It is replaced by a fairly strong warming in this area in May when, however, a cooling appears at the northwestern, southwestern, and eastern periphery of Europe. Another large-scale cooling occurs in Central, Northern, and Northwestern Europe in mid-June; it extends to the Alpine region by the end of June. Some of these minor warming holes were already noticed, although mostly not explicitly discussed, in regional trend analyses with a monthly resolution: Brázdil et al. (2009) and Rebetez and Reinhard (2008) for Central Europe, del Río et al. (2007) for the Iberian Peninsula, and Jaagus et al. (2014) for Estonia.

3.5. Localization of peak warmings

In addition to warming holes, it is also interesting to examine periods when a strong warming occurs. Although the seasonal trend analyses localize the strongest warming in Europe to winter (Cahynová and Huth, 2009; Franke et al., 2004; Jenkins et al., 2008; Klein Tank et al., 2005; Weber et al., 1997), our analysis with a higher temporal resolution suggests that in various parts of Europe, including Central and Western Europe and the Central and Western Mediterranean, a particularly strong warming occurs in other seasons: in early spring (the beginning of March), late spring (May), and late summer (August). It is in August that the largest share of stations (up to 50%) undergo significant warming for 10-, 20-, and 30-day sliding seasons (Fig. 5). The spatial structure of 30-day sliding TX trends is documented for the periods of a peak warming in Fig. 10. The strongest wintertime warming occurs around the middle of January; it peaks in Eastern Europe. Note that even in the period of the strongest warming, stations in the Eastern Mediterranean, at the Black Sea coast, and in Iceland undergo a cooling, though insignificant. Another period of a strong warming, extending over almost entire Europe, peaks in early March, together with the warming hole over Iceland and the Eastern

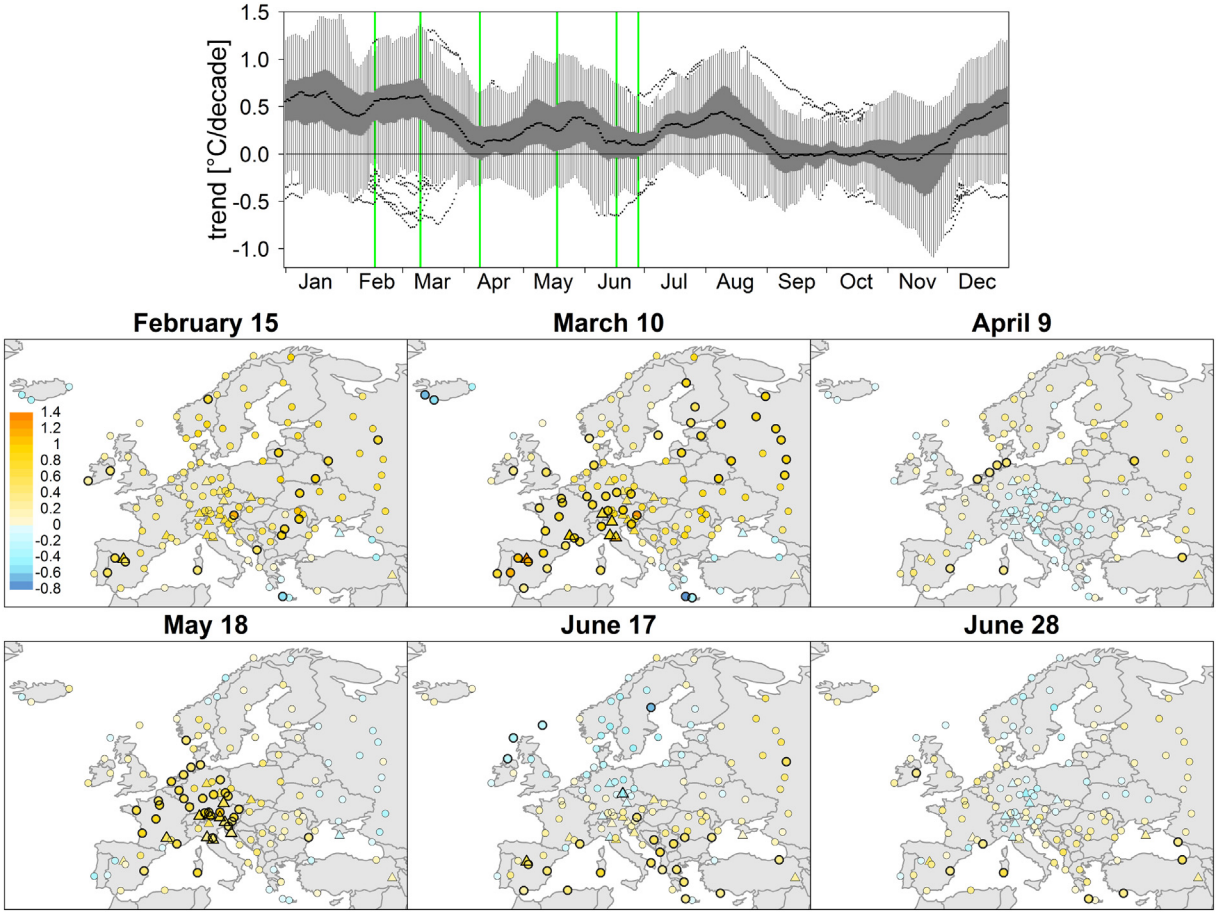

Fig. 9. Peaks of minor warming holes for TX. Display as in Fig. 8.

Mediterranean (see the central top panel in Fig. 9). The strong warming events in mid-May and early August share a similar spatial structure with the warming concentrating in Central and Western Europe.

The warming in January is even more pronounced in TN than in TX in Northern and Eastern Europe (see red and brown clusters in Fig. 6). This is illustrated by 30-year sliding TN trends for the period centered on January 18 in Fig. 11. Another region and period where and when TN trends considerably exceed TX trends is Northern Europe in the second half of March (brown cluster in Fig. 6 and Fig. 11), in particular in the Scandinavian interior and near the Gulf of Bothnia.

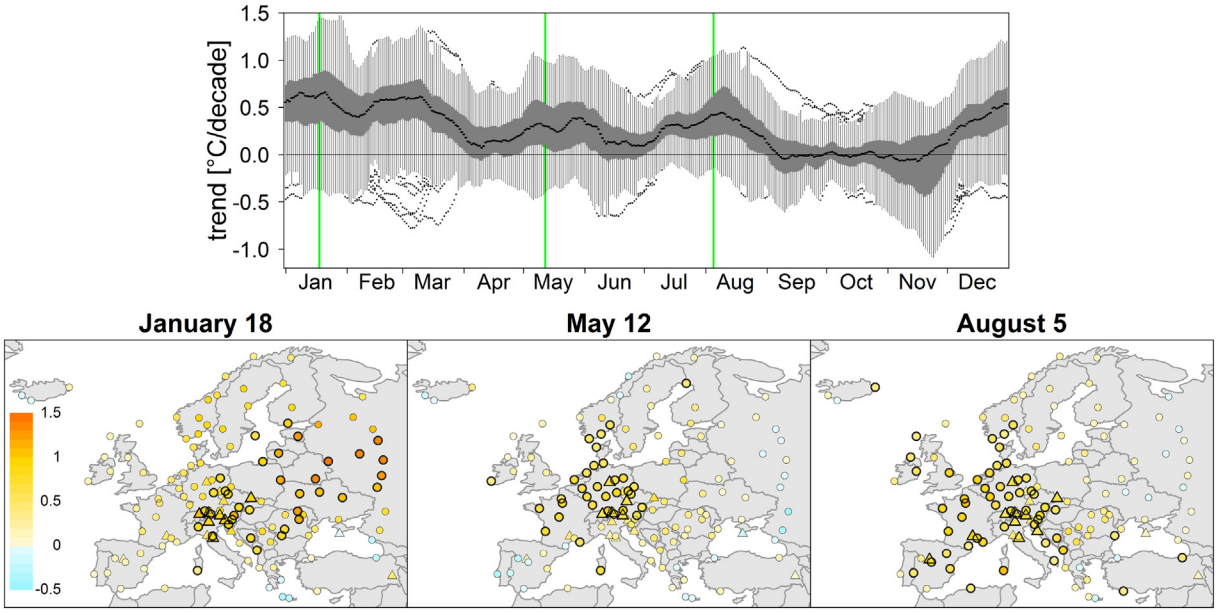

Fig. 10. Peaks of strong warming events in TX. Display as in Fig. 8. Note that another strong warming event is observed around March 10, which coincides with a minor warming hole; see Fig. 9.

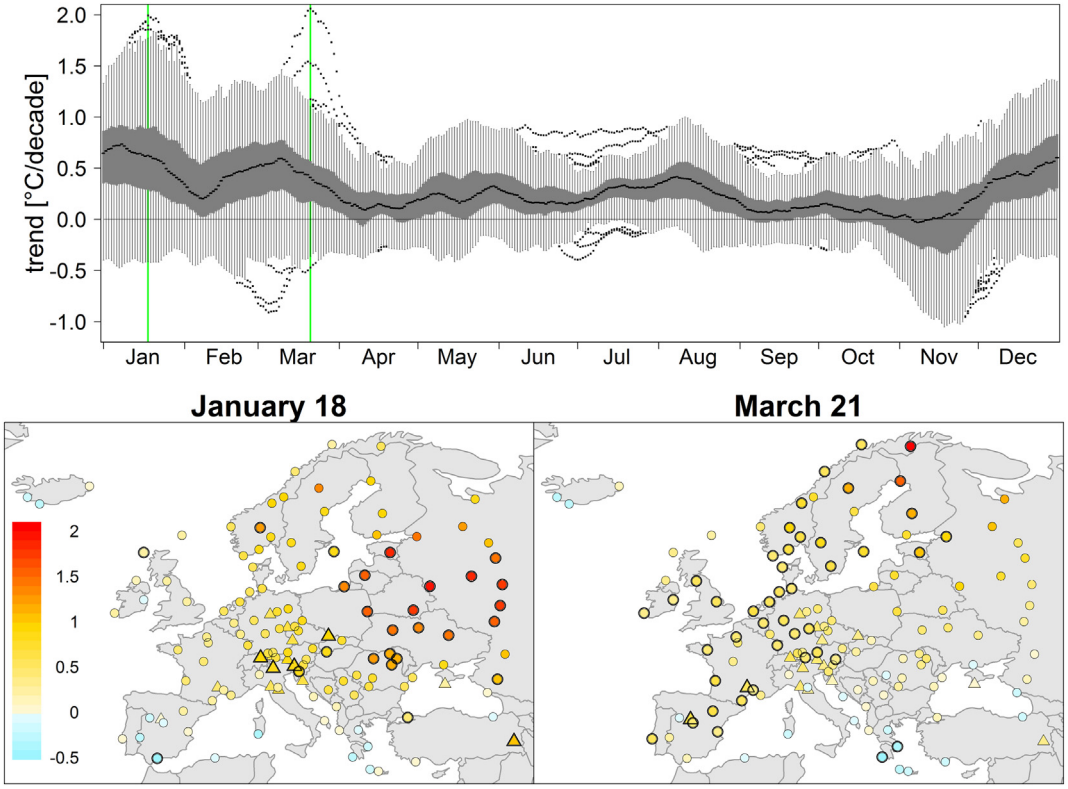

Fig. 11. Peaks of strong warming events in TN. Display as in Fig. 8 except for TN.

3.6. Magnitude of trends versus interannual variability

The highest rate of warming, of up to 1.5 °C per decade for 30-day sliding periods, is detected in Northern Europe, particularly in TN near the Baltic Sea in March, and at inland stations of the Iberian Peninsula in January. Most of these locations have continental climate, which tends to be accompanied, among others, with a large interannual variability of temperature. The association of strong temperature trends with large temperature variability is demonstrated for TX trends at four Scandinavian stations, which represent both coastal (Takle, Tromsø) and inland (Abjorsbraten, Karasjok) locations and their distance in the north-south direction is > 1000 km (Fig. 12a). The largest trends occur at the inland stations in winter (January in Abjorsbraten, February to March in Karasjok; Fig. 12c). However, winter is noted for a large interannual temperature variability at these stations (Fig. 12b). As a result, if the trends are standardized by the interannual standard deviation (Fig. 12d), the January and February trends at the inland stations no longer jut out: they become comparable to the weaker trends at the coastal stations and in summer.

The effect of interannual temperature variability on trends must be kept in mind when one compares locations with a different degree of continentality. The maritime sites typically have lower variability, hence trends attain their significance at lower magnitudes there than at continental sites. For example, trends standardized by the interannual standard deviation indicate that the relative warming (relative to temperature variability) in both TX and TN in winter is approximately the same in all regions except Iceland, the Eastern Mediterranean, and the Black Sea region; this is illustrated in Figs. S8 and S9 in supplementary material where standardized trends at all stations are shown for TX and TN, respectively. Similarly, late summer warming of TX and TN becomes, after standardization, comparable in Western, Southern, and Central Europe although the absolute magnitude is largest in Central Europe.

4. Discussion

4.1. Benefit of sliding seasons of varying length

This study introduces two novel aspects into trend analyses: the seasons over which data are averaged have varying length (from 10 to 90 days) and are sliding during the year; that is, we do not limit ourselves to calendar seasons and months.

The shorter duration of seasons allows a more precise localization of various trend features, such as warming holes and strong warming events, within the annual cycle. Whereas 90-day sliding seasons suggest a simple pattern of prevalent warming from December to August, interrupted by a period of a spatially extensive cooling in autumn, which peaks near mid-October (Fig. 5), shorter seasons clearly indicate that the two major periods are not uniform: The prevalent warming is interspersed by several short periods of more frequent cooling mainly in April and June and the autumn cooling is similarly interspersed by several short periods of more prevalent warming. The ability of short seasons to better localize the trend features is, however, at the expense of statistical significance of trends: The total number of statistically significant trends is smallest for the shortest seasons (10-days), although the magnitudes of trends are largest, and grows with the increasing length of seasons. The signal-to-noise ratio is obviously smallest for the 10-day seasons.

The sliding trends proved to be useful in describing time development of notable trend events as well as assessing representativeness of ordinary trend analyses based on fixed calendar seasons and months. Our analysis, for example, uncovers different background of the large winter warming in Western and Central Europe on one hand and in Eastern Europe on the other, as illustrated in Fig. 13 for TN. Trends for standard winter season (i.e., 90-day season centered on January 15) indicate an almost ubiquitous warming, covering entire Europe except for a few stations in the Central Mediterranean, Black Sea region, and Iceland (Fig. 13 top). The warming rate exceeds 0.4 °C per decade at most stations, reaching its peak of over 1.6 °C per decade in Tartu

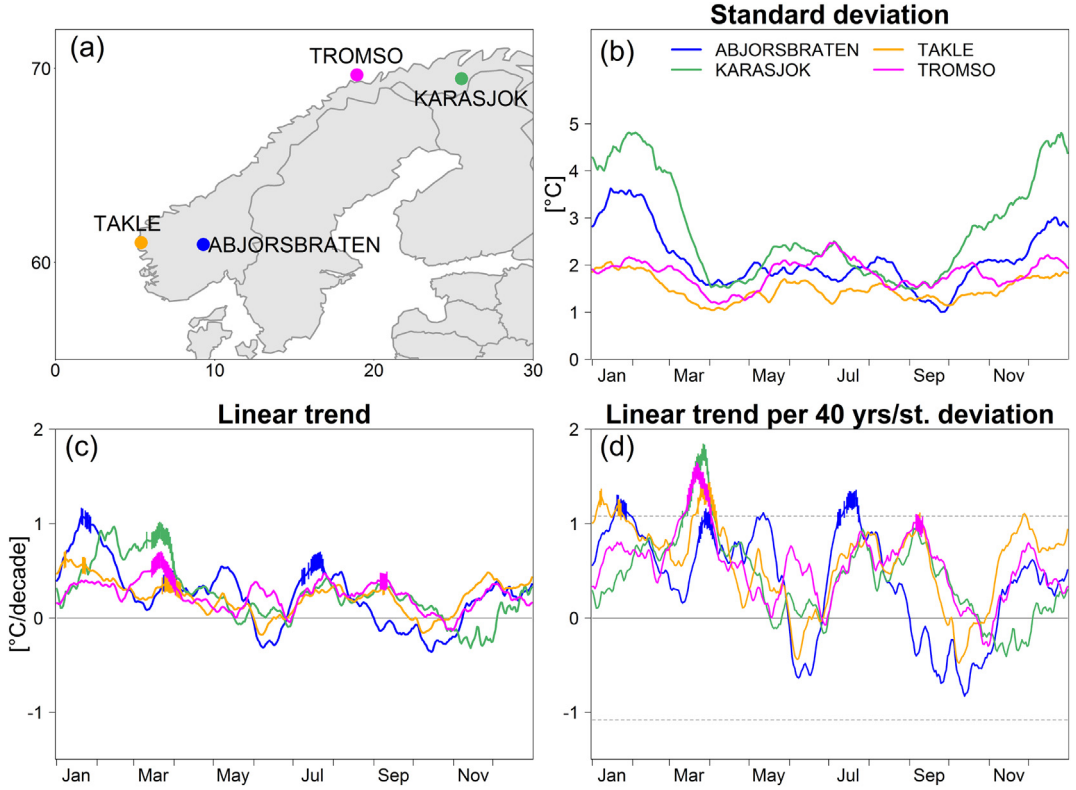

Fig. 12. Illustration of the effect of variability on the magnitude of trends, all for TX: (a) map of stations; (b) standard deviation of averages of 30-day sliding seasons (in ˚C); (c) trend magnitudes (in ˚C per decade), the format is same as in Fig. 7; (d) trends standardized by interannual standard deviation (i.e., values from (c) divided by values from (b)), dashed lines indicating the 5% statistical significance level according to *t*-test, vertical bars indicating the 5% statistical significance according to Mann-Kendall test.

(Estonia), with trends at almost 60% of stations being significant. Whereas the major contribution to the winter warming in Western and Central Europe comes from significant trends around the turn of December and January (see the 30-day trends centered on December 20 and January 5 in the bottom part of Fig. 13), the warming in Eastern Europe arises from the strong trends of almost 2 ˚C per decade in January, which extend to the second half of February at many sites. Another example of the utility of sliding trends is a seemingly continuous warming of TX and TN in all seasons in the British Isles, reported e.g. by Jenkins et al. (2008), which in fact is disrupted by two warming holes, one in early June and the other in October (Figs. 7 and S5 for TX and TN, respectively).

In a similar vein, we are able to identify several short lasting warming holes occurring in some parts of Europe in spring and summer. They could not, however, be spotted in ordinary trend analyses based on seasonal means, which suggested the warming in spring and summer was continuous (e.g., de Luis et al., 2014; Espírito Santo et al., 2014; Huth and Pokorná, 2005; Jenkins et al., 2008; Jones and Moberg, 2003; Klein Tank et al., 2005).

The analysis using sliding seasons is also able to uncover sharp temporal changes from a strong warming to cooling and vice versa. The transition from May to June is characterized by an alternation of the sign of temperature trends in many regions (Iceland, Northern Europe, Western and Eastern Mediterranean, see Fig. 7). A similar transition can be observed around the end of summer in Northern, Central, and Southeastern Europe, particularly for TX. Such fast changes are hardly detectable by an ordinary trend analysis for calendar seasons or months unless the change happens to occur near the turn of seasons or months.

4.2. Possible mechanisms of trends

Large variations of trends both in space and during year raise a question on potential mechanisms governing the trends. For local (typically within-cluster) differences, local and regional peculiarities can be blamed, including different land cover and its changes in the course of time (Beier et al., 2012; Fall et al., 2010, 2011). Larger-scale (between-cluster) differences are more difficult to attribute. There are several large-scale mechanisms that may be considered as potential contributors to the between-cluster differences. The first one is atmospheric circulation. Several studies indicate that the effect of long-term changes of atmospheric circulation on temperature trends in various parts of Europe is minor in winter and fairly small to almost negligible in other seasons (Cahynová and Huth, 2009, 2016; Ceppi et al., 2012; Fleig et al., 2015; Horton et al., 2015; Saffioti et al., 2016; van Oldenborgh and van Ulden, 2003). In spite of that, the effect of circulation cannot be dismissed entirely, especially for short sliding seasons where random variations in circulation on short-term (synoptic) scales may play a role. Another reason is that some of the above studies examined circulation effects on significant trends only; however, the contribution of circulation can be larger to insignificant trends where variability is relatively large compared to the trend magnitude. Another potential cause is the decline of Arctic sea ice; the hypothesis of its effect on temperature trends in Europe has, however, been denied by Li et al. (2015). Some studies suggest specific mechanisms for particular trend events; e.g., Otterman (2002) attribute late winter and early spring warming, manifested in earlier arrival of spring, to strengthened southwesterly winds. Such studies, however, do not form a firm framework that would explain trends throughout year and across Europe. A possible explanation of near-zero temperature changes at seaside stations in Iceland, Scotland, and Eastern Mediterranean (mostly grouped in the turquoise cluster in Fig. 6) in winter is a decrease of sea surface temperature in the North Atlantic in 1950–1990 consistent with the positive phase of the Atlantic Multidecadal Oscillation (Cannaby and Hüsrevoğlu, 2009) and generally negative sea surface temperature

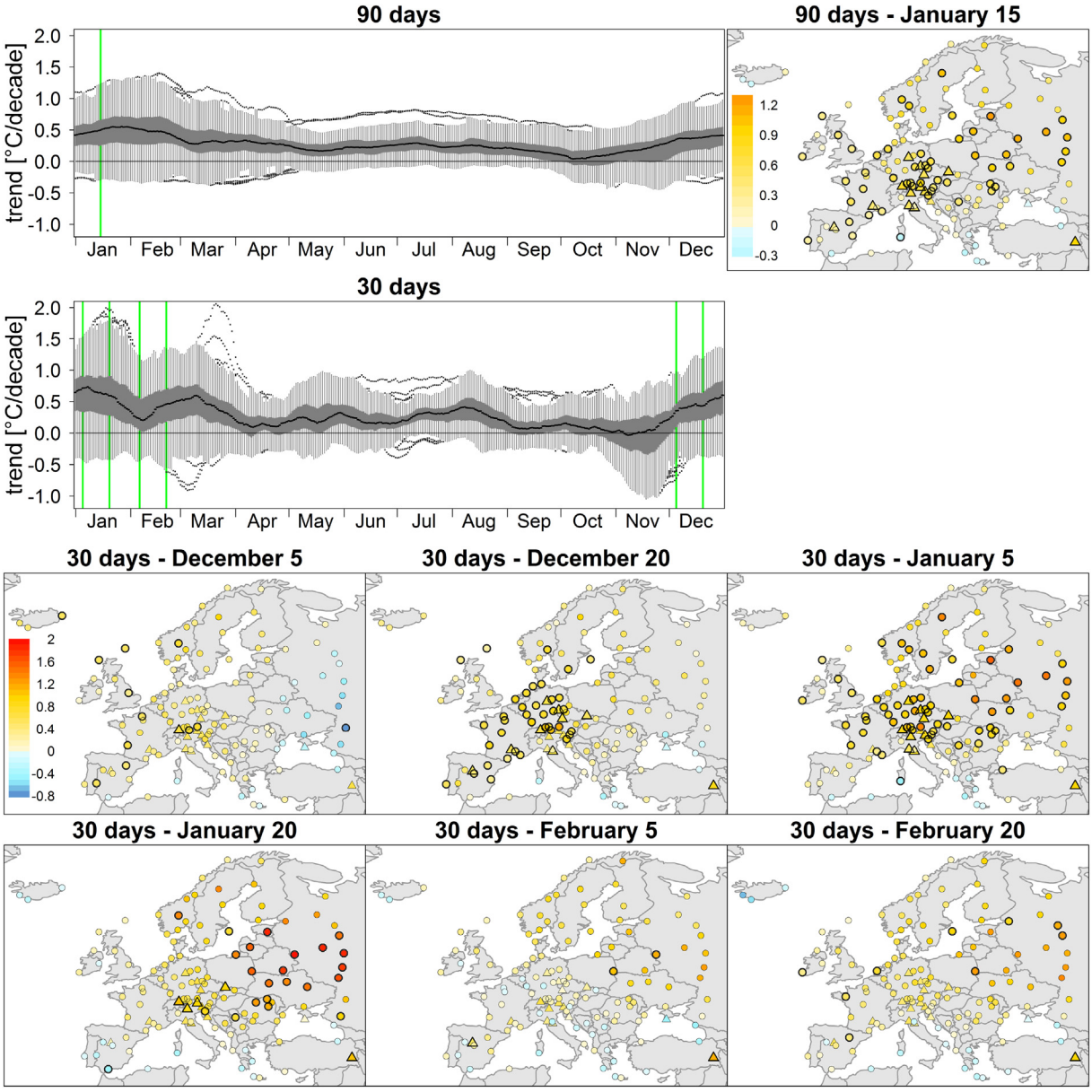

Fig. 13. Trends (°C per decade) in TN for the 90-day sliding season centered on January 15, which corresponds to winter, and selected 30-day sliding seasons in winter. Boxplots as in Fig. 2. Green vertical lines show the position of the selected days.

trends in the second half of the 20th century in both the northern North Atlantic and the Mediterranean Sea (Casey and Cornillon, 2001). Large trends of TN in winter in the proximity of the Gulf of Bothnia, described in Sec. 3.5, may at least partly result from a tendency to an earlier melt of the Baltic Sea.

Several mechanisms have been suggested as possible causes of the U.S. warming hole, including internal climate variability (Kunkel et al., 2006), sea surface temperature variations in the Atlantic (Kumar et al., 2013) and Pacific (Meehl et al., 2012, 2015; Robinson et al., 2002; Wang et al., 2009) basins, urbanization and irrigation (Misra et al., 2012), hydrological feedbacks (Pan et al., 2004, 2013), and increasing aerosol concentrations (Leibensperger et al., 2012; Banerjee et al., 2017). The wide range of candidate mechanisms and the lack of consensus on their relevance to the formation of the U.S. warming hole may stem from the fact that different mechanisms may operate in different seasons (or their parts) and in different affected regions (Mascioli et al., 2017). This suggests that a trend detection analysis that is not limited to fixed seasons and fixed regions is a suitable (and possibly necessary) first step towards the identification of mechanisms staying behind any warming hole, or more generally, behind any trend event. Neither warming holes nor other trend events in Europe have been examined in a consistent manner for their causes so far; what mechanisms stay behind them remains unclear, therefore, and is waiting for further investigations, which would require climate modeling tools. Our analysis, which is not limited to fixed seasons and fixed regions, may provide a guidance to such studies on what parts of the year and which regions to concentrate.

4.3. Trend significance

One might argue that we over-interpret our results because only a minority of trends are statistically significant (or, more precisely said, significantly different from zero). We believe that this is not the case, for at least three reasons. First, as emphasized by Nicholls (2001) and Moberg and Jones (2005), even the insignificant trends are likely to contain relevant information; by ignoring them, one is at risk of losing

it. Second, the lack of significance may not be an indication of the absence of a trend; it may rather reflect the fact that the time series is simply too short for a real trend to fully emerge from noise and become significant. The third argument is related to spatial autocorrelation and the concept of field (global, collective) significance. Trends at a certain number of stations may appear to be significant just by chance; under spatial autocorrelation, the number of randomly occurring significant trends may be even larger (e.g., Livezey and Chen, 1983; Wilks, 2016). However, even a relatively large spatial autocorrelation of temperature means of sliding seasons cannot result in the large numbers of significant trends that we observe. In a similar vein, even under a large spatial autocorrelation, the prevalence of trends of one sign, regardless of their significance, in specific periods over such a large area as Europe is highly unlikely to occur by mere chance.

4.4. Choice of period

The choice of the period (1961–2000) was dictated by the availability of sufficiently complete data series in a sufficiently dense and spatially uniform station network. The availability of fairly complete temperature series in the ECA&D database declines since the first decade of the 21st century towards present. The most recent period, noted for a slowdown of global warming (warming hiatus; e.g., Yan et al., 2015), accompanied by a considerable change in the seasonality of trends in Europe (resumed warming in autumn, cooling in winter; e.g., Li et al., 2015), is not analyzed, therefore.

It is important to realize that results of trend analysis may be very sensitive to exact start and end dates of the analyzed period (e.g., Liebmann et al., 2010). The exact timing of the warming holes, strong warming events, and other trend features would be different if the most recent period were considered; the current analysis, nevertheless, benefits from the possibility of comparisons with other trend studies, which typically analyze periods ending near the turn of centuries.

5. Conclusions

We present the analysis of how trends of minimum and maximum temperature in Europe in period 1961–2000 vary during year. The full description of the annual cycle of trends is made possible thanks to the novel concept of sliding seasons: Instead for fixed calendar seasons or months, trends are calculated for all periods of the given length (10, 20, 30, 60, and 90 days), sliding by a one day step. This allows the identification and description of trend features, such as warming holes, strong warming events, and sharp transitions of trend magnitudes over short sections of the annual cycle (several days), and their precise localization in space as well as within the annual cycle. We demonstrate that the traditional approach to trend detection, which is based on calendar seasons and months, is unable to detect most of these trend features and to localize them with sufficient precision, and can, therefore, be considered inadequate and insufficient. The trend analysis using sliding seasons is applicable to other climate elements and in other regions; we believe it may provide new insights into the occurrence and timing of important trend events, including the American warming hole.

The network of 135 stations, covering Europe as uniformly as possible, is subject to cluster analysis, with the objective to identify groups of stations with a similar annual cycle of the trends. The annual cycles of trends appear to be geographically coherent; the stations jutting out from a context of their neighbors by different amplitudes of trends in some parts of year point to possible local peculiarities of stations or data problems (inhomogeneity).

Warming is prevalent in Europe throughout year. In spite of that, in every period of year, for every sliding season of any length, there are stations with negative temperature trends. The cooling is most spatially extensive and longest in autumn, its peak values reaching −1 °C per decade; shorter and less extensive periods of cooling also appear in winter and spring. Strongest warming, with the amplitude of about 1.5 °C per decade for 30-day sliding trends, occurs in winter and early spring in Northern Europe and in the interior of the Iberian Peninsula. The identification of important trend events, such as strong warmings and warming holes, and their localization within annual cycle, is the necessary first step to be made before investigations into their specific causes can be launched, for which not only observational, but also modeling tools will be needed.

Supplementary data to this article can be found online at https://doi.org/10.1016/j.gloplacha.2018.08.015.

Acknowledgements

The study was supported by the Czech Science Foundation, project 16-04676S.

References

Bajat, B., Blagojević, D., Kilibarda, M., Luković, J., Tošić, I., 2016. Spatial analysis of the temperature trends in Serbia during the period 1961–2010. Theor. Appl. Climatol. 121, 289–301. https://doi.org/10.1007/s00704-014-1243-7.

Banerjee, A., Polvani, L.M., Fyfe, J.C., 2017. The United States "warming hole": Quantifying the forced aerosol response given large internal variability. Geophys. Res. Lett. 44, 1928–1937. https://doi.org/10.1002/2016GL071567.

Beier, C.M., Signell, S.A., Luttman, A., Degaetano, A.T., 2012. High-resolution climate change mapping with gridded historical climate products. Landsc. Ecol. 27, 327–342. https://doi.org/10.1007/s10980-011-9698-8.

Brázdil, R., 1996. Trends of maximum and minimum daily temperatures in central and southeastern Europe. Int. J. Climatol. 16, 765–782.

Brázdil, R., Chromá, K., Dobrovolný, P., Tolasz, R., 2009. Climate fluctuations in the Czech Republic during the period 1961–2005. Int. J. Climatol. 29, 223–242. https://doi.org/10.1002/joc.1718.

Cahynová, M., Huth, R., 2009. Changes of atmospheric circulation in Central Europe and their influence on climatic trends in the Czech Republic. Theor. Appl. Climatol. 96, 57–68. https://doi.org/10.1007/s00704-008-0097-2.

Cahynová, M., Huth, R., 2016. Atmospheric circulation influence on climatic trends in Europe: an analysis of circulation type classifications from the COST733 catalogue. Int. J. Climatol. 36, 2743–2760. https://doi.org/10.1002/joc.4003.

Cannaby, H., Hüsrevoğlu, Y.S., 2009. The influence of low-frequency variability and long-term trends in North Atlantic Sea surface temperature on Irish waters. ICES J. Mar. Sci. 66, 1480–1489. https://doi.org/10.1093/icesjms/fsp062.

Casey, K.S., Cornillon, P., 2001. Global and regional sea surface temperature trends. J. Clim. 14, 3801–3818. https://doi.org/10.1175/1520-0442(2001)014<3801:GARSST>2.0.CO;2.

Cavanaugh, N.R., Shen, S.S.P., 2014. Northern Hemisphere climatology and trends of statistical moments documented from GHCN-Daily surface air temperature station data from 1950 to 2010. J. Clim. 27, 5396–5410. https://doi.org/10.1175/JCLI-D-13-00470.1.

Ceppi, P., Scherrer, S.C., Fischer, A.M., Appenzeller, C., 2012. Revisiting Swiss temperature trends 1959–2008. Int. J. Climatol. 32, 203–213.

de Luis, M., Čufar, K., Saz, M.A., Longares, L.A., Ceglar, A., Kajfež-Bogataj, L., 2014. Trends in seasonal precipitation and temperature in Slovenia during 1951–2007. Reg. Environ. Chang. 14, 1801–1810. https://doi.org/10.1007/s10113-012-0365-7.

del Río, S., Fraile, R., Herrero, L., Penas, A., 2007. Analysis of recent trends in mean maximum and minimum temperatures in a region of the NW of Spain (Castilla y Leon). Theor. Appl. Climatol. 90, 1–12. https://doi.org/10.1007/s00704-006-0278-9.

Domonkos, P., Tar, K., 2003. Long-term changes in observed temperature and precipitation series 1901–1998 from Hungary and their relations to large scale changes. Theor. Appl. Climatol. 75, 131–147. https://doi.org/10.1007/s00704-002-0716-2.

Drijfhout, S., van Oldenborgh, G.J., Cimatoribus, A., 2012. Is a decline of AMOC causing the warming hole above the North Atlantic in observed and modeled warming patterns? J. Climate 25, 8373–8379. https://doi.org/10.1175/JCLI-D-12-00490.1.

Dumitrescu, A., Bojariu, R., Birsan, M.-V., Marin, L., Manea, A., 2015. Recent climatic changes in Romania from observational data (1961–2013). Theor. Appl. Climatol. 122, 111–119. https://doi.org/10.1007/s00704-014-1290-0.

Easterling, D.R., 1997. Maximum and minimum temperature trends for the globe. Science 277, 364–367.

El Kenawy, A., López-Moreno, J.I., Vicente-Serrano, S.M., 2012. Trend and variability of surface air temperature in northeastern Spain (1920–2006): Linkage to atmospheric circulation. Atmos. Res. 106, 159–180. https://doi.org/10.1016/j.atmosres.2011.12.006.

Espírito Santo, F., de Lima, M.I.P., Ramos, A.M., Trigo, R.M., 2014. Trends in seasonal surface air temperature in mainland Portugal, since 1941. Int. J. Climatol. 34, 1814–1837. https://doi.org/10.1002/joc.3803.

Fall, S., D. Niyogi, A. Gluhovsky, R. A. Pielke, E. Kalnay, and G. Rochon, 2010 Impacts of land use land cover on temperature trends over the continental United States: assessment using the north American Regional Reanalysis. Int. J. Climatol., 30, 1980–1993.

Fall, S., Watts, A., Nielsen-Gammon, J., Jones, E., Niyogi, D., Christy, J.R., Pielke, R.A.,

2011. Analysis of the impacts of station exposure in the U.S. Historical Climatology Network temperatures and temperature trends. J. Geophys. Res. 116, D14120. https://doi.org/10.1029/2010JD015146.
Falvey, M., Garreaud, R.D., 2009. Regional cooling in a warming world: recent temperature trends in the Southeast Pacific and along the west coast of subtropical South America (1979–2006). J. Geophys. Res. 114, D04102. https://doi.org/10.1029/2008JD010519.
Feidas, H., Makrogiannis, T., Bora-Senta, E., 2004. Trend analysis of air temperature time series in Greece and their relationship with circulation using surface and satellite data: 1955–2001. Theor. Appl. Climatol. 79, 185–208. https://doi.org/10.1007/s00704-016-1854-2.
Fleig, A.K., Tallaksen, L.M., James, P., Hisdal, H., Stahl, K., 2015. Attribution of European precipitation and temperature trends to changes in synoptic circulation. Hydrol. Earth Syst. Sci. 19, 3093–3107. https://doi.org/10.5194/hess-19-3093-2015.
Franke, J., Goldberg, V., Eichelmann, U., Freydank, E., Bernhofer, C., 2004. Statistical analysis of regional climate trends in Saxony, Germany. Clim. Res. 27, 145–150. https://doi.org/10.3354/cr027145.
Hartmann, D.L., 2013. Observations: atmosphere and surface. climate change 2013: the physical science basis. In: Stocker, T.F. (Ed.), Contribution of Working Group I to the Fifth Assessment Report of the Intergovernmental Panel on Climate Change. Cambridge University Press, pp. 159–254.
Horton, D.E., Johnson, N.C., Singh, D., Swain, D.L., Rajaratnam, B., Diffenbaugh, N.S., 2015. Contribution of changes in atmospheric circulation patterns to extreme temperature trends. Nature 522, 465–469. https://doi.org/10.1038/nature14550.
Hu, Z.Z., Yang, S., Wu, R.G., 2003. Long-term climate variations in China and global warming signals. J. Geophys. Res. Atmos. 108, 4614. https://doi.org/10.1029/2003JD003651.
Huth, R., Pokorná, L., 2004. Parametric versus non-parametric estimates of climatic trends. Theor. Appl. Climatol. 77, 107–112. https://doi.org/10.1007/s00704-003-0026-3.
Huth, R., Pokorná, L., 2005. Simultaneous analysis of climatic trends in multiple variables: an example of application of multivariate statistical methods. Int. J. Climatol. 25, 469–484. https://doi.org/10.1002/joc.1146.
Huth, R., Nemešová, I., Klimperová, N., 1993. Weather categorization based on the average linkage clustering technique: an application to European mid-latitudes. Int. J. Climatol. 13, 817–835.
Jaagus, J., Briede, A., Rimkus, E., Remm, K., 2014. Variability and trends in daily minimum and maximum temperatures and in the diurnal temperature range in Lithuania, Latvia and Estonia in 1951–2010. Theor. Appl. Climatol. 118, 57–68. https://doi.org/10.1007/s00704-013-1041-7.
Jenkins, G.J., Perry, M.C., Prior, M.J., 2008. The Climate of the United Kingdom and Recent Trends. Met Office Hadley Centre, Exeter, UK.
Jones, P.D., 1995. Maximum and minimum temperature trends in Ireland, Italy, Thailand, Turkey and Bangladesh. Atmos. Res. 37, 67–78.
Jones, P.D., Moberg, A., 2003. Hemispheric and large-scale surface air temperature variations: an extensive revision and an update to 2001. J. Clim. 16, 206–223.
Karl, T.R., et al., 1993. A new perspective on recent global warming: Asymmetric trends of daily maximum and minimum temperature. Bull. Amer. Meteor. Soc. 74, 1007–1023.
Kaufman, L., Rousseeuw, P.J., 1990. Finding Groups in Data: An Introduction to Cluster Analysis. John Wiley & Sons, New York.
Keevallik, S., Russak, V., 2001. Changes in the amount of low clouds in Estonia (1955–1995). Int. J. Climatol. 21, 389–397.
Klein Tank, A.M.G., 2002. Daily dataset of 20th-century surface air temperature and precipitation series for the European climate Assessment. Int. J. Climatol. 22, 1441–1453. https://doi.org/10.1002/joc.773.
Klein Tank, A.M.G., Können, G.P., Selten, F.M., 2005. Signals of anthropogenic influence on European warming as seen in the trend patterns of daily temperature variance. Int. J. Climatol. 25, 1–16. https://doi.org/10.1002/joc.1087.
Klok, E.J., Klein Tank, A.M.G., 2009. Updated and extended European dataset of daily climate observations. Int. J. Climatol. 29, 1182–1191. https://doi.org/10.1002/joc.1779.
Kruger, A.C., Shongwe, S., 2004. Temperature trends in South Africa: 1960–2003. Int. J. Climatol. 24, 1929–1945. https://doi.org/10.1002/joc.1096.
Kumar, S., Kinter III, J., Dirmeyer, P.A., Pan, Z., Adams, J., 2013. Multidecadal climate variability and the "warming hole" in North America: results from CMIP5 twentieth- and twenty-first-century climate simulations. J. Clim. 26, 3511–3527. https://doi.org/10.1175/JCLI-D-12-00535.1.
Kunkel, K.E., Liang, X.Z., Zhu, J., Lin, Y., 2006. Can CGCMs simulate the twentieth-century "warming hole" in the Central United States? J. Climate 19, 4137–4153. https://doi.org/10.1175/JCLI3848.1.
Lanzante, J.R., 1996. Resistant, robust and non-parametric techniques for the analysis of climate data: Theory and examples, including applications to historical radiosonde station data. Int. J. Climatol. 16, 1197–1226.
Leibensperger, E.M., Mickley, L.J., Jacob, D.J., Chen, W.-T., Seinfeld, J.H., Nenes, A., Adams, P.J., Streets, D.G., Kumar, N., Rind, D., 2012. Climatic effects of 1950-2050 changes in US anthropogenic aerosols – part 2: climate response. Atmos. Chem. Phys. 12, 3349–3362. https://doi.org/10.5194/acp-12-3349-2012.
Li, C., Stevens, B., Marotzke, J., 2015. Eurasian winter cooling in the warming hiatus of 1998–2012. Geophys. Res. Lett. 42, 8131–8139. https://doi.org/10.1002/2015GL065327.
Liebmann, B., Dole, R.M., Jones, C., Bladé, I., Allured, D., 2010. Influence of choice of time period on global surface temperature trend estimates. Bull. Amer. Meteorol. Soc. 91, 1485–1491. https://doi.org/10.1175/2010BAMS3030.1.
Livezey, R.E., Chen, W.Y., 1983. Statistical field significance and its determination by Monte Carlo techniques. Mon. Weather Rev. 111, 46–59.
Mamara, A., Argiriou, A.A., Anadranistakis, M., 2016. Recent trend analysis of mean air temperature in Greece based on homogenized data. Theor. Appl. Climatol. 126, 543–573. https://doi.org/10.1007/s00704-015-1592-x.
Mascioli, N.R., Previdi, M., Fiore, A.M., Ting, M.F., 2017. Timing and seasonality of the United States 'warming hole'. Envion. Res. Lett. 12, 034008. https://doi.org/10.1088/1748-9326/aa5ef4.
Meehl, G.A., Arblaster, J.M., Branstator, G., 2012. Mechanisms contributing to the warming hole and the consequent U.S. east-west differential of heat extremes. J. Clim. 25, 6394–6408. https://doi.org/10.1175/JCLI-D-11-00655.1.
Meehl, G.A., Arblaster, J.M., Chung, C.T.Y., 2015. Disappearance of the southeast U.S. "warming hole" with the late 1990s transition of the Interdecadal Pacific Oscillation. Geophys. Res. Lett. 42, 5534–5570. https://doi.org/10.1002/2015GL064586.
Misra, V., Michael, J.-P., Boyles, R., Chassignet, E.P., Griffin, M., O'Brien, J.J., 2012. Reconciling the spatial distribution of the surface temperature trends in the southeastern United States. J. Clim. 25, 3610–3618. https://doi.org/10.1175/JCLI-D-11-00170.1.
Moberg, A., Jones, P.D., 2005. Trends in indices for extremes in daily temperature and precipitation in central and western Europe. Int. J. Climatol. 25, 1149–1171. https://doi.org/10.1002/joc.1163.
Moliba, J.C., Huth, R., Beranová, R., 2006. Roční chod trendů klimatických prvků v ČR. (annual cycle in trends of climatic elements in the Czech Republic). Meteorol. zpr. 59, 129–134.
Nicholls, N., 2001. The insignificance of significance testing. Bull. Am. Meteorol. Soc. 82, 981–986. https://doi.org/10.2307/3802789.
Ohmura, A., 2012. Enhanced temperature variability in high-altitude climate change. Theor. Appl. Climatol. 110, 499–508. https://doi.org/10.1007/s00704-012-0687-x.
Otterman, J., 2002. Are stronger North-Atlantic southwesterlies the forcing to the late-winter warming in Europe? Int. J. Climatol. 22, 743–750. https://doi.org/10.1002/joc.681.
Pan, Z., Arritt, R.W., Takle, E.S., Gutowski, W.J., Anderson, C.J., Segal, M., 2004. Altered hydrologic feedback in a warming climate introduces a "warming hole". Geophys. Res. Lett. 31, L17109. https://doi.org/10.1029/2004GL020528.
Pan, Z.T., Liu, X.D., Kumar, S., Gao, Z.Q., Kinter, J., 2013. Intermodel variability and mechanism attribution of central and southeastern U.S. anomalous cooling in the twentieth century as simulated by CMIP5 models. J. Clim. 26, 6215–6237. https://doi.org/10.1175/JCLI-D-12-00559.1.
Philipona, R., 2013. Greenhouse warming and solar brightening in and around the Alps. Int. J. Climatol. 33, 1530–1537. https://doi.org/10.1002/joc.3531.
Rangwala, I., Miller, J.R., 2012. Climate change in mountains: a review of elevation-dependent warming and its possible causes. Clim. Chang. 114, 527–547. https://doi.org/10.1007/s10584-012-0419-3.
Rebetez, M., Reinhard, M., 2008. Monthly air temperature trends in Switzerland 1901–2000 and 1975–2004. Theor. Appl. Climatol. 91, 27–34. https://doi.org/10.1007/s00704-007-0296-2.
Robinson, W.A., Ruedy, R., Hansen, J.E., 2002. General circulation model simulations of recent cooling in the east-Central United States. J. Geophys. Res. 107 (D24), 4748. https://doi.org/10.1029/2001JD001577.
Rogers, J.C., 2013. The 20th century cooling trend over the southeastern United States. Clim. Dyn. 40, 341–352. https://doi.org/10.1007/s00382-012-1437-6.
Saffioti, C., Fischer, E.M., Scherrer, S.C., Knutti, R., 2016. Reconciling observed and modeled temperature and precipitation trends over Europe by adjusting for circulation variability. Geophys. Res. Lett. 43, 8189–8198. https://doi.org/10.1002/2016GL069802.
Scherrer, S.C., Appenzeller, C., Liniger, M.A., 2006. Temperature trends in Switzerland and Europe: Implications for climate normals. Int. J. Climatol. 26, 565–580. https://doi.org/10.1002/joc.1270.
Scherrer, S.C., Ceppi, P., Croci-Maspoli, M., Appenzeller, C., 2012. Snow-albedo feedback and Swiss spring temperature trends. Theor. Appl. Climatol. 110, 509–516. https://doi.org/10.1007/s00704-012-0712-0.
Serquet, G., Marty, C., Dulex, J.P., Rebetez, M., 2011. Seasonal trends and temperature dependence of the snowfall/precipitation-day ratio in Switzerland. Geophys. Res. Lett. 38, L07703. https://doi.org/10.1029/2011GL046976.
Serra, C., Burgueno, A., Lana, X., 2001. Analysis of maximum and minimum daily temperatures recorded at Fabra observatory (Barcelona, NE Spain) in the period 1917–1998. Int. J. Climatol. 21, 617–636. https://doi.org/10.1002/joc.633.
Sneyers, R., 1990. On the Statistical Analysis of Series of Observation. WMO, Geneve, pp. 192 Technical note No. 143.
The R Project for Statistical Computing Accessed 29 June 2012. [Available online at http://www.r-project.org/.]
van Oldenborgh, G.J., van Ulden, A., 2003. On the relationship between global warming, local warming in the Netherlands and changes in circulation in the 20th century. Int. J. Climatol. 23, 1711–1724. https://doi.org/10.1002/joc.966.
van Oldenborgh, G.J., Drijfhout, S., van Ulden, A., Haarsma, R., Sterl, A., Severijns, C., Hazeleger, W., Dijkstra, H., 2009. Western Europe is warming much faster than expected. Clim. Past 5, 1–12. https://doi.org/10.5194/cp-5-1-2009.
Wang, H., Schubert, S., Suarez, M., Chen, J., Hoerling, M., Kumar, A., Pegion, P., 2009. Attribution of the seasonality and regionality in climate trends over the United States during 1950–2000. J. Clim. 22, 2571–2590. https://doi.org/10.1175/2008JCLI2359.1.
Weber, R.O., Talkner, P., Stefanicki, G., 1994. Asymmetric diurnal temperature change in the Alpine region. Gephys. Res. Lett. 21, 673–676.
Weber, R.O., Talkner, P., Auer, I., Böhm, R., Gajić-Čapka, M., Zaninović, K., Brázdil, R., Faško, P., 1997. 20th-century changes of temperature in the mountain regions of Central Europe. Clim. Chang. 36, 327–344.
Wibig, J., Glowicki, B., 2002. Trends of minimum and maximum temperature in Poland. Clim. Res. 20, 123–133. https://doi.org/10.3354/cr020123.

Wilks, D.S., 2016. The stippling shows statistically significant gridpoints: How research results are routinely overstated and overinterpreted, and what to do about it. Bull. Am. Meteorol. Soc. 97, 2263–2273. https://doi.org/10.1175/BAMS-D-15-00267.1.

Xoplaki, E., Luterbacher, J., Paeth, H., Dietrich, D., Steiner, N., Grosjean, M., Wanner, H., 2005. European spring and autumn temperature variability and change of extremes over the last half millennium. Geoph. Res. Lett. 32, L15713. https://doi.org/10.1029/2005GL023424.

Yan, X.-H., Boyer, T., Trenberth, K., Karl, T.R., Xie, S.-P., Nieves, V., Tung, K.-K., Roemmich, D., 2015. The global warming hiatus: Slowdown or redistribution? Earth's Future 4, 472–482. https://doi.org/10.1002/2016EF000417.

Zhang, X., Vincent, L.A., Hogg, W.D., Niitsoo, A., 2000. Temperature and precipitation trends in Canada during the 20th Century. Atmosphere-Ocean 38, 395–429. https://doi.org/10.1080/07055900.2000.9649654.